Universidade do Minho

Escola de Engenharia

Beatriz Sousa Afonso

Scale-up production of food grade nanoparticles aiming their application in food products

Mestrado Integrado em Engenharia Biológica
Ramo de Tecnologia Química e Alimentar

Trabalho efetuado sob orientação do:
Professor Doutor Eugénio Manuel Faria Campos Ferreira
e do supervisor na empresa:
Doutor Miguel Ângelo Parente Ribeiro Cerqueira

Janeiro de 2020

AGRADECIMENTOS

Gostaria de expressar o meu sincero obrigada a todos que contribuíram, direta ou indiretamente, para a realização deste trabalho. Posso dizer com muito orgulho que cresci imenso com esta experiência, tanto a nível intelectual como pessoal.

Primeiramente, quero agradecer ao meu supervisor do INL, Doutor Miguel Cerqueira, pela mentoria, pela disponibilidade e pela oportunidade de fazer parte de uma grande equipa de investigadores e me ter permitido uma experiência extremamente enriquecedora.

Também, quero agradecer a uma contribuição essencial neste trabalho, Gabriela Azevedo, Catarina Gonçalves e Isabel Rodriguez pela ajuda incansável, pela paciência, prontividade em ajudar e disponibilidade.

Ao meu orientador, Professor Eugénio Ferreira, por me clarificar dúvidas, apoiar neste trabalho e dedicação do seu tempo.

Quero agradecer aos meu colegas do INL por me terem acolhido de forma tão especial e por tornarem esta experiência uma memória que guardo com muito carinho.

Por fim, e com uma consideração especial, à minha família e aos meus amigos por terem contribuído para todo o meu percurso académico com muito apoio e incentivo.

O desenvolvimento deste trabalho foi ainda realizado ao abrigo do Projeto "MobFood – Mobilização de conhecimento científico e tecnológico em resposta aos desafios do mercado Agroalimentar" (POCI-01-0247-FEDER-024524), pelo Consórcio "MobFood", financiado pelo Fundo Europeu de Desenvolvimento Regional (FEDER), através do Sistema de Incentivos à Investigação e Desenvolvimento Tecnológico, no âmbito do Programa Operacional para a Competitividade e Internacionalização do Portugal2020.

Cofinanciado por:

STATEMENT OF INTEGRITY

I hereby declare having conducted this academic work with integrity. I confirm that I have not used plagiarism or any form of undue use of information or falsification of results along the process leading to its elaboration.

I further declare that I have fully acknowledged the Code of Ethical Conduct of the University of Minho.

RESUMO

Nanopartículas poliméricas são estruturas promissoras para o encapsulamento de vários materiais, com o objetivo de proteger o composto bioativo e libertação no local desejado.

Este trabalho tem como objetivo a avaliação de mecanismos de aumento de escala para a produção de nanopartículas poliméricas e testar a sua exequibilidade a nível laboratorial para uma aplicação futura a nível industrial. Assim sendo, diferentes mecanismos foram investigados: misturador em forma de T, nanoprecipitação flash e através da utilização de uma membrana. Deste modo, o equipamento mais promissor a escalamento será o misturador em forma de T, capaz de um escalamento até 20 vezes a escala laboratorial e mais fácil de contruir.

À escala laboratorial, foram produzidas nanopartículas, através do método de nanoprecipitação, capazes de encapsular β–caroteno, um composto hidrofóbico lipofílico e sensível à luz testando dois polímeros distintos como material de parede: zeína e etilcelulose. Em seguimento, foram caracterizadas por vários métodos e foi realizada uma simulação gastrointestinal *in vitro*.

Os resultados da produção a nível laboratorial mostram que as condições ótimas para uma produção de nanopartículas com distribuição de tamanho reduzida e controlada são concentrações baixas de polímero e concentrações altas de anti-solvente. Para o nanossistema etilcelulose-β-caroteno, foi usada a concentração de 0,0004% de β-caroteno (BC) para produzir nanopartículas com tamanho (por intensidade) de 59,9 nm, PDI de 0,274, eficiência de encapsulação de 66,56% e potencial zeta de -96 mV exibindo comportamento estável. No nanossistema zeína- β-caroteno, a concentração de 0,001% de β-caroteno foi usada para produzir as nanopartículas, resultando em tamanhos de 82,7 nm, PDI de 0,286, eficiência de encapsulamento de 92,69% e potencial zeta de +70,5 mV.

Por fim, os resultados obtidos da digestão *in vitro* demonstraram que ambos os polímeros melhoraram a libertação de BC no local desejado quando comparado com o controlo (BC livre em óleo). No entanto, nenhum dos polímeros apresentou um valor de bioacessibilidade elevado, com 11,78% e 14,89% para as nanopartículas de etilcelulose e de zeína, respetivamente na fase intestinal. Ambos os polímeros melhoraram a estabilidade química do β-caroteno, retardando a sua libertação na fase gástrica. Contudo, a zeína foi o polímero que apresentou melhores valores de bioacessibilidade.

Palavras chave: Misturador em forma de T, β–caroteno, Etilcelulose, Zeína, nanoprecipitação

ABSTRACT

Polymeric nanosystems are promising structures for the encapsulation of various materials with the goal of protecting the bioactive compound and delivery at the target site.

This work has as final goal the assessment of scale-up techniques for the production of polymeric nanoparticles, testing its feasibility at a lab-scale for the future application at an industrial scale. Therefore, several mechanisms were investigated: T-mixer, flash nanoprecipitation and membrane contactor. The nanoparticles were produced at a laboratory scale to evaluate their feasibility using the solvent-displacement method. Thus, being the most promising technique using a T mixer device, able to a 20-fold scale-up and easier to fabricate.

At laboratory scale, nanoparticles were produced, through the solvent-displacement method, with the ability to encapsulate β–carotene, a hydrophobic lipophilic light sensitive compound. Two different polymers were used as encapsulating materials: zein and ethylcellulose. Then, the nanoparticles were characterized by several methods and an *in vitro* gastrointestinal simulation was performed.

Results show that the best conditions for a size-controlled production of nanoparticles with a narrow size distribution are lower polymer concentrations and higher antisolvent concentrations. For the ethylcellulose-β–carotene system, a concentration of 0.0004% of β–carotene was used to produce nanoparticles with size by intensity of 59.9 nm, PDI of 0.274, encapsulation efficiency of 66.56% and high stability behavior with a zeta potential of – 93.26 mV. In the zein-β–carotene system, a concentration of 0.001% of β–carotene was used to produce the nanoparticles, resulting in sizes of 82.7 nm, PDI of 0.286, encapsulation efficiency reaching 92.69% and zeta potential of + 70.5 mV.

Lastly, results obtained from the *in vitro* digestion demonstrated that both polymers have improved release of BC at the target site comparing to the control sample of free BC in oil. However, none of the polymers showed high bioaccessibility, having 11.78 % and 14.89 % for the ethylcellulose nanoparticles and zein nanoparticles, respectively in the intestinal phase. Both polymers improved chemical stability of entrapped beta-carotene by retarding its release in the gastric phase. Nonetheless, zein was the polymer with better results for the bioaccessibility.

Key words: T mixer, β–carotene, Ethylcellulose, Zein, Solvent-displacement

TABLE OF CONTENTS

LIST OF FIGURES

LIST OF TABLES

LIST OF NOMENCLATURE

EC – ethylcellulose

BC –β-carotene

GRAS – generally recognized as safe

PLA – poly(lactic acid)

PLGA – poly(lactic-*co*-glycolic acid)

DLS — Dynamic Light Scattering

EE — Encapsulation Efficiency

FTIR — Fourier Transform Infrared

TEM — Transmission Electron Microscopy

XRD — X-ray Diffraction

SD — Standard Deviation

NPs — nanoparticles

FNP — Flash Nanoprecipitation

CIJM — Confined Impingement Jet Mixer

MIVM — Multi-Inlet Vortex Mixer

CHAPTER 1 INTRODUCTION

1.1 Motivation

Currently, consumers have a growing interest in foods that can help in a healthy lifestyle and prevent illness. This demand has led to the development of new and innovative functional foods that are enriched and fortified with new ingredients beyond their basic nutrition (Wan et al., 2015).

Carotenoids are pigments naturally present in plants and β-carotene is known for its provitamin A function and antioxidant capacity (Packer, Kraemer et al. 2005). Therefore, this compound can be used as a dietary supplement in foods. However, adding pure bioactive compounds directly to foods may present a challenge due to their physicochemical properties and therefore resulting in limited biological activity (Wan et al., 2015). In the case of β-carotene, their direct use in foods is limited by the poor water-solubility, chemical instability and low bioavailability leading to a poor intake by the body (Qian et al, 2012). For these reasons, the development of a food-grade delivery system that enables the encapsulation of β-carotene and therefore its incorporation in food products is a solution of great interest.

The production of delivery systems able to encapsulate bioactive compounds is only mastered at laboratory-scale. However, the amount produced at laboratory-scale is not enough to fulfil the requirements of the consumers. Thus, there is a need to optimize a system that allows the production of larger quantities of nanoparticles containing a bioactive compound to be incorporated in food products. Research centers and companies have been developing methods for their large-scale production (Gunstone, 2003).

1.2 Approach

This work aimed to design polymeric nanoparticles loaded with β-carotene and improve its bioaccessibility. The polymers tested were ethylcellulose and zein. Since β-carotene is a hydrophobic compound, the designed carriers were prepared to improve its bioaccessibility, protecting it from the harsh conditions of the digestion process.

For this purpose, both ethylcellulose and zein nanoparticles were prepared following the solvent-displacement method (nanoprecipitation). Then, the final particles were submitted to several tests to assess their functionality and morphology. An *in vitro* simulation of the digestion process was carried out to evaluate the bioaccessibility of β-carotene after digestion representing the amount of β-carotene that would be available for intestinal absorption.

This work also presents a review of scale-up strategies for the production of the produced food-grade polymeric nanoparticles based on the solvent-displacement method.

1.3 Nanoencapsulation in food products

Nanotechnology has a great potential to improve the quality and safety of foods. When applied to the food industry can be used to modify some of the food characteristics, such as stability during shelf life, coloring strength, texture and taste. (Silva et al., 2012)

Nano can play a major role in incorporating bioactive ingredients such as carotenoids, polyphenols, vitamins and minerals into food products (Wan et al., 2015). For that purpose, food-grade polymer nanoparticles as carriers of bioactive ingredients have been used as delivery systems for controlled release and the protection of these ingredients against adverse conditions present in the human body (Fernandez et al., 2009)

The encapsulation of bioactive ingredients may be achieved in nanoparticles with different structural features, namely i) nanospheres, that are homogeneous matrix particles having their entire arrangement solid, constituted only by the polymer where active compounds can be trapped inside, dissolved in it or adsorbed at the sphere surface, ii) nanocapsules, that are non-homogeneous vesicles having a polymeric shell surrounding a liquid core in which the active compounds are dissolved but may also be absorbed in the surface of the capsule (Pinto Reis et al., 2006; Vauthier & Bouchemal, 2009)

The encapsulation of bioactive compounds offers a wide range of solutions in the food industry in terms of health, safety and high-quality products (Barreras-Urbina et al., 2016). Improved solubility and bioavailability are achieved due to the controlled release of functional compounds targeting specific sites of action, in particular compounds with poor solubility in certain matrices. The protective capsule masks astringency tastes, having less impact on the sensory attributes of foods and the bioactive compound is sheltered from degradation from the conditions it can be exposed (Lepeltier et al., 2015).

1.4 β-carotene

In recent years, there has been a growing interest in foods that provide health benefits. These so-called functional foods provide added benefits beyond the basic nutrition of the initial food product. Therefore, secondary plant metabolites namely, carotenoids, are promising ingredients to be incorporated in foods due to their proposed health benefits.

There are more than 60 different carotenoids present in vegetable products that are consumed by humans. Among them, the most common are β-carotene, lutein, zeaxanthin and lycopene (Dasgupta & Klein, 2014; Gunstone, 2003). Carotenoids are naturally occurring pigments that absorb blue and purple light with maxima at 450 nm (Pénicaud et al., 2011) thus displaying the color red, orange and yellow, responsible for the bright colors of many vegetables (Gunstone, 2003). They are held in the chloroplasts as oil droplets, for instance in fruits (Alminger et al., 2014). β-carotene can be found predominantly in vegetables and fruits such as cantaloupe, carrots, mangos, sweet potatoes and several greens (spinach, lettuce) (Boon et al., 2010; Gunstone, 2003).

β-carotene is fat-soluble and best-known for its function as a natural antioxidant and high pro-vitamin A activity (Packer et al., 2005). It comprises properties such as the ability to scavenge active free radicals, neutralizing peroxy radicals as well as singlet oxygen, thus protecting cellular tissues from lipid peroxidation (Dasgupta & Klein, 2014; Paiva & Russell, 1999). It is oxidized by light due to the presence of conjugated double bounds in their molecules functioning as light-harvesting pigments and photoprotective agents in vegetables (Gunstone, 2003).

β-carotene is currently being used as a food additive with the European denomination E160 (European Comission, 2008) acting as a coloring agent, antioxidant and vitamin A capacities (de Freitas Zômpero et al., 2015).

Structurally, β-carotene is constituted by a polyene chain with 11 conjugated double bounds and two rings at each end of the chain (Wang et al., 2018).

As a provitamin A carotenoid, it can be cleaved by the enzyme β-carotene 15,15' monooxygenase present in the human intestine and liver to form two equivalent retinol molecules (Pénicaud et al., 2011). Vitamin A designate the group of compounds such as retinol, retinal, retinoic acid and retinyl esters. The enzyme acts when the body is in need for vitamin A, using β-carotene as a form of vitamin A. If the body has sufficient vitamin then β-carotene will be stored for futures needs or

absorbed intact. For vitamin A, 1 IU corresponds to 0.0006 mg of β-carotene (Dasgupta & Klein, 2014).

The properties that gives carotenoids beneficial properties in healthy body function creates challenges when carotenoids are added to food products. Because of β-carotene hydrophobic character, it is insoluble in water and displays poor bioavailability in crystalline form thus making it difficult the absorption through diet (Yusuf et al., 2012). β-carotene is slightly soluble in ethanol. Três et al. (2007) predicted its solubility at 0.360 mg/mL at 20 °C.

Bioaccessibility of a certain compound is intended to be the portion of the nutrient from the food that is available for absorption, the amount that is released from the food matrix during digestion and accessible for absorption into the mucosa (Hedrén, Diaz, & Svanberg, 2002). Much attention has focused on β-carotene bioaccessibility due to several factors that might influence it, such as solubility, the viscosity of the medium, interactions with other compounds present in the food matrix (e.g. competition with other fat-soluble nutrients such as vitamin E), the food processing method applied and the presence of factors that interfere with micelle formation (Hedrén et al., 2002; Paiva & Russell, 1999).

Encapsulation

Encapsulation of labile compounds has been a solution for many challenges in the food industry. β-carotene displays several limiting factors that hinder its use in food products in its free form. Those limitations consist of water insolubility, light, oxygen and heat sensitivity, chemical instability and low bioavailability (Deng et al., 2014; Wang et al., 2018). Also, they limit the amount of β-carotene to reach the specific sites where its action is needed (Chuacharoen & Sabliov, 2016). The bioaccessibility of carotenoids from raw vegetables is approximately 10% (Ribeiro et al., 2008).

A compelling approach to protect and deliver labile ingredients is to incorporate them within a coating or wall material (Deng et al., 2014). Said nanoparticles can be developed into polymer-based systems that allow a controlled release of β-carotene and help decrease their degradation (Boon et al., 2010). *In vitro*, *ex vivo* and *in vivo* experiments proved that β-carotene nanostructures are superior to pure β-carotene (Jain et al., 2018).

There are diversified methods to design β-carotene nanoparticles. Those include the microencapsulation of β-carotene with soy protein isolate and OSA-modified starch by one of the most common techniques which is spray-drying (Deng et al., 2014). Through emulsion-

electrospray, β-carotene particles were made within zein and whey protein concentrate to improve bioaccessibility (Gómez-Mascaraque et al., 2017). Furthermore, homogenization-evaporation method was employed to produce β-carotene nanoparticles with different protein materials (Yi, Lam, et al., 2015). Solvent-displacement (or nanoprecipitation) was also performed with different wall material such as PLA, PLGA (Ribeiro et al., 2008), sodium caseinate (Yin, et al., 2009) and zein (Chuacharoen & Sabliov, 2016).

Health related properties

A diet with a large consumption of fruits and vegetables rich in β-carotene is less likely to develop lung cancer, cardiovascular diseases or age-related macular degeneration (Albanes, 1999; Gunstone, 2003). Once β-carotene is converted to vitamin A, the health benefits derived from the vitamin comprise the maintenance of normal eye health and immune system function, an important role in cell differentiation and organ development (Boon et al., 2010). β-carotene supplementation can be also be used to treat patients with a photosensitive disorder (Packer et al., 2005).

Despite all the benefits stated above, β-carotene supplementation in a high-risk population, such as smokers and asbestos-exposed workers did not show protective effects against cancer or cardiovascular diseases (Boon et al., 2010; Paiva & Russell, 1999). The environment of the lungs of smokers have lower circulating concentrations of antioxidants, among them is β-carotene (Dasgupta & Klein, 2014). This environment enhances β-carotene breakdown to produce oxidative by-products that may induce lung carcinogenesis (Packer et al., 2005).

β-carotene does not have recommended dietary allowance, however, the recommendation for vitamin A for women and men is 800 and 1000 μg of retinol (or retinol equivalents), respectively. Assuming that all β-carotene consumed is converted to retinol the dietary allowance would be approximately 4.8 and 6.0 mg for women and men, respectively (Albanes, 1999). The dietary allowance of vitamin A is expressed in retinol equivalents due to the existence of two sources: preformed vitamin from animal products such as animal tissues, milk and eggs and provitamin A from carotenoids in vegetables and fruits. Most of the humans are omnivores and consume a mixture of the two sources of the vitamin. However, consuming high doses of vitamin A from animal products can cause hypervitaminosis but the overconsumption of β-carotene foods is tightly regulated in which the body only converts the vitamin needed, storing or absorbing the remaining β-carotene (Packer et al., 2005). As previously stated, risk groups can be harmed by ingesting β-

carotene, which may result in increased lung cancer. Nonetheless, it does not exhibit toxicity or a health hazard in non-at-risk groups. When ingested in large amounts, can cause the appearance of carotenoderma, i.e., the accumulation of β-carotene in the skin giving it a yellow or orange tone (Packer et al., 2005).

1.5 Polymers

The polymers used to produce the food-grade nanoparticles have to fulfill certain requirements regarding food safety. they must be non-toxic, non-immunogenic and biodegradable or at least totally eliminated from the body without any risk of accumulation, and its degradation products must follow the same requirements (Vauthier & Bouchemal, 2009). In the US they have to be selected from the materials granted GRAS (generally recognized as safe) status (Wan et al., 2015), and in the EU they must be approved for food use as ingredient, additive of novel food.

1.5.1 Ethylcellulose

Ethylcellulose is a non-toxic, water-insoluble, biodegradable polymer used in the development of a variety of polymer nanoparticles (Urbán-Morlán et al., 2015). It is a semisynthetic material having properties such as wall-forming and biocompatibility (Avanço & Braschi, 2008). Moreover, it is a tasteless, white to light tan-colored powder which has a wide range of applications in the food, cosmetic and pharmaceutical fields (Lai, Pitt, & Craig, 2010; Rowe et al., 2009).

Cellulose derivatives possess the polymeric backbone of cellulose, which contains a basic repeating structure of anhydroglucose units, each unit comprises three replaceable hydroxyl groups (Rekhi & Jambhekar, 1995).

Ethylcellulose (EC) is produced via etherification of alkali cellulose using ethyl chloride. Figure 1.2 shows the structure of ethylcellulose, where it can be seen the anhydroglucose unit which has the three reactive hydroxyl groups ethoxylated (Porter, 1989). The repeating anhydroglucose units (n) are modified into ethyl ether groups to form the so-called ethyl ether of cellulose or ethylcellulose. The number of units joined by acetal linkages can vary to provide a wide variety of molecular weights (Rowe et al., 2009). The physical properties of EC are determined by the main chain properties such as the degree of polymerization and by the side-chain properties such as degree of substitution and the distribution of these substituents (Lai et al., 2010).

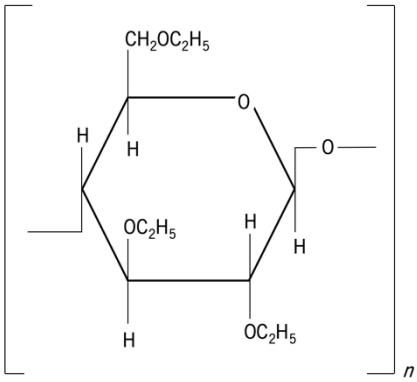

Figure 1.1. Molecular structure of ethylcellulose. Image adapted from (Rekhi & Jambhekar, 1995).

Ethylcellulose is soluble in a wide variety of solvents such as esters, aromatic hydrocarbons, alcohols, ketones and chlorinated solvents. It is also soluble in ethanol and methanol yielding solutions with lower viscosity (Rekhi & Jambhekar, 1995). Moreover, EC is insoluble in water, therefore it is widely used for the controlled release of hydrophobic bioactive compounds (Murtaza, 2012).

Ethylcellulose materials vary according to the degree of etherification or ethoxyl substitution, which is measured by the ethoxyl content. These materials are also produced in different viscosity grades of differing molecular weight: the higher the polymer molecule chain the higher is the viscosity (Rekhi & Jambhekar, 1995; Rowe et al., 2009). It can range from 7 to 100 mPas (7-100 cP), however for controlled release purposes, higher EC viscosities formulations resulted in slower drug release rates, while lower viscosities formulation resulted in the fastest drug release rate (Murtaza, 2012; Rowe et al., 2009). Ultimately, for the assemble of nanoparticles with the goal of controlled release of ingredients the optimal conditions combine a lower concentration of ethylcellulose with a lower viscosity ethylcellulose formulation.

Applications

The growing interest in renewable polymer resources, as opposed to petroleum-based polymers and chemicals, leads to an increasing importance of cellulose ethers handling. Among cellulose derivatives, ethylcellulose applications go from a coating material to a thickening agent (Rekhi & Jambhekar, 1995).

Several uses have been reported for this polymer, as well as a wide range of fields of application. It is most widely used in the pharmaceutical field for a number of functions such as a viscosity

increasing agent and film former (Rowe et al., 2009); a hydrophobic coating agent in the release of a drug to mask unpleasant taste, improve the stability, control odor or taste, protect drugs from moisture or oxidation and to alter solubility or prevent incompatibilities (Avanço & Braschi, 2008; Murtaza, 2012); in topical formulation EC is used as a thickening agent for creams, lotions and gels (Rowe et al., 2009); and in the food industry as a stabilizer for emulsions and as an emulsifier (Rowe et al., 2009)

Safety

Several synthetic polymers have been used to formulate delivery systems, and for its application in foods they need to be approved. EC is approved as a food additive in Europe (E462) (European Comission, 2008), considered GRAS and approved by the FDA as safe for human consumption and it is included in the Canadian List of Acceptable Non-medicinal Ingredients (Rowe et al., 2009)

Nanoparticles

Literature shows that ethylcellulose can be used to encapsulate compounds with different properties and that a great variety of methods can be used to produce those nanoparticles. Among those methods, the most used in the literature, are the production of nanoparticles by solvent-displacement (or nanoprecipitation) (Fessi, et al., 1989), by solvent evaporation (Avanço & Braschi, 2008; Leitner et al., 2019), and by water-in-oil-in-oil double emulsion solvent diffusion method (Rama, Senapati, & Das, 2005). Some of the works with ethylcellulose nanoparticles comprise encapsulation of drugs such as ciclosporin, taxol, betaxolol, essential oils, lipiodol (contrast agent) (Fessi et al., 1989), zidovudine (Rama et al., 2005), ibuprofen (Swathi & Krishna Sailaja, 2014) and biobased photoprotectants (Hayden et al., 2018).

1.5.2 Zein

Corn is mainly composed by the endosperm and germ, which are where the proteins are mainly located (Anderson & Lamsal, 2011). There are several types of proteins on corn, which represents approximately 10% of the dry mass. However, zein proteins comprise about 80% of the whole protein content (Papalia & Londero, 2015). Zein belongs to the group of corn proteins named prolamins (Patent No. US 9,381,252 B2, 2016; Zhang, Cui, Che, et al., 2015) and it is not constituted by a single protein but a mixture of four different classes grouped by solubility and sequence similarity, it can be divided into α-, β-, γ- and δ-zeins. α-zein is the most abundant fractions, approximately 80% of the total zein mass (Li et al., 2017).

Zein is an amphiphilic biopolymer since it has both hydrophobic and hydrophilic attributes. The hydrophobic aminoacid content is represented by leucine, proline and alanine and the hydrophilic counterpart is represented by glutamine (Corradini et al., 2014). However, zein almost completely lacks lysine and tryptophan amino acids which is why it has poor nutritional quality (Patent No. US 9,381,252 B2, 2016; Holding, 2014). The combination of zein's different amino acids is responsible for its particular solubility: zein is insoluble in pure water and in pure ethanol, making it a material of interest for the controlled release of a loaded compound, but is soluble in aqueous-ethanol solutions at certain concentrations (Hurtado-López & Murdan, 2005; Jain et al., 2018). It is also soluble in mixtures of water with aliphatic alcohols and other organic solvents containing hydroxyls, carbonyls, amines and other polar groups (Corradini et al., 2014).

Commercial zein is usually extracted from corn gluten, which is a renewable source, through the conventional process of aqueous-alcohol extraction (Anderson & Lamsal, 2011). The extract is then centrifuged and chilled to precipitate the zein. At last, it is dried and form a yellowish powder (Corradini et al., 2014).

Zein is a renewable, biodegradable and biocompatible (Corradini et al., 2014) powder with a yellow color due to the carotenoids (β–carotene, zeaxanthin and lutein) present in the corn (Sessa et al., 2003). In addition, is thermally stable up to 280 °C, shows great oxygen barrier properties (Corradini et al., 2014; Penalva et al., 2017) and can withstand gastric pH (Zhang et al., 2016).

Applications

Zein has been investigated as carriers in various forms such as nanoparticles, films, hydrogels, micelles and nanofibers (Zhang, Cui, Chen, et al., 2015; Zhang et al., 2016) with several purposes being used for controlled release, improved stability of bioactive agents, controlled delivery and enhanced oral bioavailability of bioactive agents (Zhang, Cui, Che, et al., 2015; Zhang et al., 2016). As a result of these properties, zein can be used for the production of adhesives, chewing gum, coating for food products, textiles, ceramic, cosmetic powders, as an encapsulator for pesticides and inks (Patent No. US 9,381,252 B2, 2016; Anderson & Lamsal, 2011; Holding, 2014). It can serve as a biodegradable and sustainable material for the replacement of oil-based plastic (Fernandez et al., 2009) and, in the food industry, zein-based nanoparticles are used for encapsulation, stabilization and controlled release of bioactive compounds such as essential oils, polyphenols, food coloring agents (Wan et al., 2015), carotenoids (Chuacharoen & Sabliov, 2016; Wang et al., 2018) and vitamins (Kasaai, 2018).

Safety

Plant-based proteins have become a material of increasing interest due to their abundance, relatively low cost in comparison with animal proteins and due to their safety (Zhang et al., 2015). Zein has been regarded with "Generally Recognized as Safe" (GRAS) status by the Food & Drug Administration (U.S. Food & Drug Administration, 2019). and it is also included in non-parenteral medicines licensed in the UK and in the Canadian List of Acceptable Non-medicinal Ingredients (Rowe et al., 2009). Therefore, it is a product considered food-grade and is safe for use in human or animal food according to the Codex Alimentarius of a country (Patent No. US 9,381,252 B2, 2016).

Nanoparticles

Zein with spherical morphology has the optimal shape for controlled release and protection of nutrients: provides a minimum contact with the environment and longest diffusion pathways (Kasaai, 2018). Zein nanoparticles has been used in the pharmaceutical and food fields, and different methods have been employed for the development of those nanoparticles. Among them are the anti-solvent precipitation (Li et al., 2017), phase separation and electrospraying (Wan et al., 2015). The distinct methods produce particles with the ability to encapsulate several bioactive compounds such as insulin (Patent No. US 9,381,252 B2, 2016), β-carotene (Chuacharoen & Sabliov, 2016; Jain et al., 2018), folic acid, resveratrol (Peñalva et al., 2015), quercetin (Penalva et al., 2017) and even essential oils (Wan et al., 2015).

1.6 Solvent Displacement Method

The solvent displacement method also known as nanoprecipitation was described by Fessi et al. (1989) and consists of the development of nanoparticles in a reproducible, easy and scalable way. Because nowadays there is an increasing interest to employ processes that are environmentally sustainable, safe and energy-saving, the solvent displacement method has been widely used. This technique enables the production of nanospheres as well as nanocapsules in one step, cost-efficient and high yield encapsulation of hydrophobic compounds (Calderó et al., 2019).

Nanoprecipitation requires three basic ingredients to be performed: the polymer, the polymer solvent and the non-solvent of the polymer (Vauthier & Bouchemal, 2009). In the selection of a suitable solvent, it has to comprise the ability of complete miscibility with the non-solvent, in addition to good solubilization of the bioactive compound and lower boiling point from the solvent,

so that removal by evaporation can occur (Horn & Rieger, 2001). Acetone is the most used solvent for this method. Other solvents such as ethanol, hexane and methylene chloride or a binary solvent blend can also be used. The polymers commonly used in this technique are PLA and PLGA (Rao & Geckeler, 2011). The polymer, the bioactive compound to be encapsulated and the solvent constitute the organic phase. The non-solvent of the polymer constitutes the aqueous phase which is usually water. Other materials could be added to this phase such as hydrophilic surfactants to avoid particles' aggregation and coating materials (Miladi, Sfar, Fessi, & Elaissari, 2016).

To produce the nanoparticles, the organic phase is poured into large amounts of aqueous phase under moderate stirring, usually with a magnetic stirrer. Reversing the order by adding large amounts of aqueous phase to the organic phase can also produce nanoparticles. When the phases come in contact, the solvent rapidly diffuses into the water, the polymer and the bioactive compound are insoluble in the mixed binary solution formed and precipitate producing nanoparticles (Rao & Geckeler, 2011). Then, the suspension of nanoparticles is submitted to evaporation to remove the organic solvent. To remove the aqueous phase so that a powder can be obtained, freeze drying can be used (Miladi et al., 2016). Several operating conditions influence the characteristics of the nanoparticles such as, the ratio of organic phase to aqueous phase, stirring rate, injection rate of the organic phase, which phase is poured and polymer concentration (Rao & Geckeler, 2011).

The particle formation in the nanoprecipitation technique can be explained by nucleation theory which involves three phases: nucleation, growth and aggregation showed by Lince et al. (2008). When a solution of a polar water-miscible solvent containing a hydrophobic solute is mixed with large amounts of water, the concentration of the solute reaches its solubility limit causing nucleation of small solute molecules. Therefore, nucleation is driven by the saturation limit, i.e., when the aqueous phase breaks the interface between polymer and solvent. Supersaturation determines nucleation rate, thus mixing has an important effect: poor mixing of phases leads to low nucleation rate and produces big nanoparticles, high nucleation rates produces large amounts of smaller particles. Growth occurs through the capture of non-aggregated solute molecules added to the core from the surrounding solution. The separation of nucleation and growth allows obtaining a uniform particle suspension. Operating conditions well controlled aim for high nucleation rates and consequently low growth rates. Aggregation occurs when the particles formed previously collide with already existing particles, forming larger aggregates. In this phase maintaining control of the

agitation rate helps prevent aggregation and achieve uniformity. The final size reached by the nanoparticles is determined by the rate of each phase (Barreras-Urbina et al., 2016; Miladi et al., 2016; Rao & Geckeler, 2011).

Moreover, Quintanar-Guerrero et al. (1998) explained how the organic phase and the aqueous phase diffuse onto each other. Based on the different surface tensions: the aqueous phase has a high surface tension (pulls strongly on the surroundings solution) and the organic phase has lower surface tension. When they mix together, interfacial turbulence is caused and leads to the formation of vortices of solvent at the interface of both liquids. The organic solvent diffuses from low surface tensions regions to the water causing gradual precipitation of the polymer and the bioactive compound within it (Miladi et al., 2016).

Advantages

The selection of a suitable method for the preparation of polymeric nanoparticles is made based on size requirement, the simplicity of the procedure, area of application and consequently safety of the materials used, the need for purification and the type of polymeric-compound system (Rao & Geckeler, 2011).

Methods for the production of polymeric nanoparticles can be described mainly in four procedures: emulsion evaporation, emulsion diffusion, salting-out and solvent displacement. All the former methods include an organic solution and an aqueous solution which may need to contain stabilizers; the methods can only encapsulate lipophilic components and they all enable the production of nanospheres. However, only solvent displacement and emulsification-diffusion produces nanocapsules (Quintanar-Guerrero et al., 1998).

Nanoprecipitation mostly differs from the other methods in that no emulsion precursor is required, being a straightforward and rapid method able to develop nanoparticles in one step and can be carried out without surfactants in the aqueous phase (Lepeltier et al., 2014). Moreover, the nanoparticles produced present sizes ranging from 50 to 300 nm, smaller sizes generate greater contact area (Barreras-Urbina et al., 2016) and it is easy to scale-up (Vauthier & Bouchemal, 2009). Some general applications of this method are the production of ibuprofen loaded ethylcellulose nanoparticles (Swathi & Krishna Sailaja, 2014) and UV-absorbing nanoparticles from ethylcellulose and zein with biobased photoprotectants (quercetin, retinol and p-coumaric acid) (Hayden et al., 2018).

CHAPTER 2 OVERVIEW OF SCALE-UP PRODUCTION OF FOOD GRADE NANOPARTICLES

2.1 Introduction

Polymeric nanoparticles have been one of the most promising drug delivery systems (Galindo-Rodríguez et al., 2005). Thus, the development of a large production process for the optimized polymeric nanoparticles has its origin in the need for the bulk production of nanoparticles for several uses, namely in the food and pharmaceutical industry. The synthesis of nanoparticles is well implemented and studied at the laboratory-scale. However, its production at an industrial scale lack information.

The pilot-scale production is the stage between the laboratory and industrial scale. It is meant to assess the drawbacks that may be present at the scaled-up stage that are not noticeable at a smaller dimension. And so, it combines the parameters that need optimization (Vauthier & Bouchemal, 2009).

Among the several nanoparticle preparation strategies, the antisolvent-precipitation method has been established as a robust and scalable method, showing good reproducibility and stable formulations (D'Addio & Prud'homme, 2011). Two other methods for the pilot-scale production of nanoparticles were performed by (Galindo-Rodríguez et al., 2005) to produce ibuprofen loaded nanoparticles: emulsification–solvent diffusion and emulsification–reverse salting out. Both of these methods are a two-step procedure and requires the formation of an emulsion. The time for each method to produce a single pilot-batch was also evaluated – from the preparation of solutions to the productions of the nanoparticles. Emulsification diffusion showed the longest time (350 min) followed by salting-out (300 min) and nanoprecipitation took 120 min. Nanoprecipitation showed to be the easier and fastest method. However, for the same volume of raw solutions used nanoprecipitation only recovered 18 mg of nanoparticles compared to 169.6 and 100.0 mg of emulsification-diffusion and salting-out methods. This is due to the disadvantage of nanoprecipitation that only allows to use low polymer concentrations. (Galindo-Rodríguez et al., 2005)

The mixing of the phases is a challenging and important step in nanoparticle formation, therefore mixing devices are widely used to produce nanoparticles (Valente et al., 2012). Several of these

devices have been used for the production of polymeric nanoparticles at laboratory-scale that are feasible to scale-up. Among them, the most promising are nanoparticles produced by a T mixer device, flash nanoprecipitation and by membrane contactor.

This overview starts by exploring the devices mostly used for the pilot-scale where the nanoprecipitation method is employed and then unfolds the several strategies and that are feasible to scale-up.

2.2 T mixer

In the antisolvent-precipitation method, one of the critical parameters is the mixing of the organic phase with the aqueous phase. This stage has a great influence on the formation of the nanoparticles, producing the precipitation and assembly of the nanoparticles. Thus, when designing the scaled-up process, a crucial step is providing the best mixing of the phases. A device with a T shape was first described by Briançon et al. (1999), which composed the central piece that would allow the phases to come in contact and diffuse into each other, with a continuous feeding process. The experimental set up consists of a total of three reactors: two reactors (A and B), each filled with stock solutions of the phases to mix and another reactor (C) to collect the nanoparticle suspension coming from the T mixer device and maintain the suspension under agitation. The two phases are then pumped using peristaltic pumps, at a determined constant flow rate to the central device and nanoparticles are formed (Briançon et al., 1999).

This set up can be continuously fed by insuring the continuous formation of nanoparticles. The volume of the nanoparticle's batches can be up to 20-fold larger compared to laboratory-scale (Vauthier & Bouchemal, 2009).

A few experimental studies have evaluated the practicality of the method. Briançon et al. (1999) achieved a batch production of 2.5 L of particles with a concentration between 0.1 to 0.3% (weight fraction) using as organic phase acrylic polymer dissolved in acetone or a mixture of acetone and isopropanol and as aqueous phase water and surfactant. Galindo-Rodríguez et al. (2005) produced ibuprofen loaded nanoparticles batch of 1.5 L using flow rates of 62.5 and 125.0 mL/min for organic phase and aqueous phase, respectively. Tewa-Tagne et al. (2007) also performed the production of nanoparticles using a T-mixer, obtaining great quantities of nanoparticles (30-fold the laboratory scale) with good reproducibility and achieving single batch production of approximately

2.25 L (polymer used was Poly(epsilon-caprolactone) and encapsulated drug was Caprilic/capric triglyceride (Miglyol 810®) with Sorbitan monostearate (Montane 60®)).

The method allows the production in a facile and reproducible way, which aids the scale-up process. Moreover, it enables the preparation of batches of different volumes, by adjusting a few parameters, namely aqueous solution flow rate and organic solution flow rate (Galindo-Rodríguez et al., 2005). For the size distribution the most important parameter to control is the polymer concentration in the initial organic phase; in fact nanoparticles' size can be controlled by modifying the composition of the phases (Briançon et al., 1999).

The main limitation of the method is the low polymer concentration to be used in the organic phase. Above the maximum concentration, the polymer tends to precipitate (e.g. in the form of films), which reduces the amount of nanoparticles recovered (Briançon et al., 1999).

2.3 Flash nanoprecipitation

Flash nanoprecipitation (FNP) technology relies on a rapid mixing of two impinging streams with equal momentum: aqueous phase with the organic phase, creating high supersaturation in a confined chamber (Tao et al., 2019). Solvent and antisolvent flash mix creating the solute nucleation, growth by coagulation and condensation until they reach a stable critical value. The mixing of the phases is achieved in milliseconds, therefore, nucleation and growth happened at the same time. If the growth prevails, the final particle suspension displays broad size distribution and large particle size. (Tao et al., 2019)

High efficiency mixers were design to obtain a homogeneous super saturated solution (Chow et al., 2015). The most common devices are FNP using confined impingement jets mixer (CIJM) developed by Johnson & Prud'homme (2003) and multi-inlet vortex mixer (MIVM) by Liu et al. (2008).

CIJM is composed by two opposing inlet jets (organic phase and aqueous phase) that are meant to collide at high velocity inside a small chamber (Figure 2.1.). Parameters such as the inlet jet diameter and the size of the mixing chamber affect the final nanoparticle size (Valente et al., 2012). Wan et al. (2015) successfully produced zein particles by Flash Nanoprecipitation using a confined impinging jet. Zein concentrations ranged between 2.5—7.5% (w/v) obtaining sizes below 350 nm and the controlled parameters were flow rate of zein solution and the outlet configuration.

Chow et al, (2015) reported the production of curcumin-loaded PEG-PLA nanoparticles using CIJM. Equal streams of organic phase and aqueous phase were injected upon another in the chamber controlled by a syringe pump, however after the mixing of the phases, the suspensions must be further diluted. The main drawback reported was the low stability of the particles' suspension, showing aggregation hours after production (Chow et al., 2015).

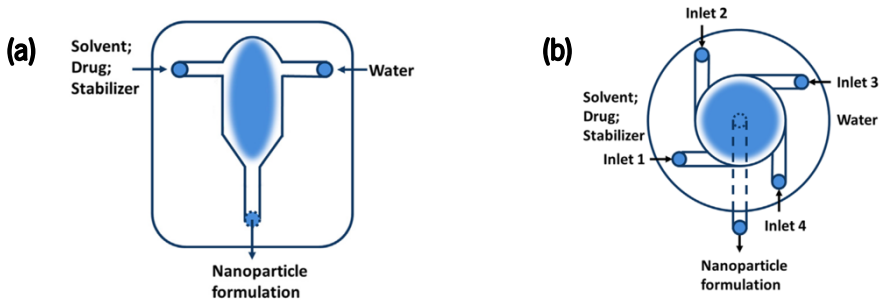

Figure 2.1. Representation of (a) confined impinging jet mixer section view, (b) multi-inlet vortex mixer top view. Image from (Tao et al., 2019).

MIVM is composed by four inlets positioned at an angle that liquid streams at high velocity collide producing a vortex (Figure 2.1). Each stream can be loaded with solvents at different ratios and materials and can be adjusted at different flow rates providing an improved control on the nanoparticles supersaturation. Moreover, the rapid mixing rates and high efficiency between organic and aqueous phase through the manipulation of flow rate and composition of the liquid streams provide faster nucleation and growth rates (D'Addio & Prud'homme, 2011; Tao et al., 2019) therefore, MIVM is easier to control particle size by different levels of supersaturation compared to CIJM.

The continuous and controllable production of ultrafine nanoparticles with good repeatability by microfluidic mixer devices makes it scale-up easily.

Flash nanoprecipitation devices provide continuous and controllable production of nanoparticles with good reproducibility which makes it a potential mechanism to scale-up from laboratory to industrial scale. In addition, the devices can be operated in parallel with several units scaled-up (Tao et al., 2019).

2.4 Membrane contactor

The membrane contactor is a technique that uses a filtration device to produce nanoparticles. The organic phase is pressed through the pores while the aqueous phase circulates tangentially inside the membrane. When the two phases come in contact the nanoparticles are assembled and dragged to the outlet (Charcosset & Fessi, 2005; Urbán-Morlán et al., 2015).

The experimental set-up includes a pump that ensures a continuous stream of the aqueous phase through the membrane. The aqueous phase vessel is maintained at constant stirring and the organic phase is placed in a pressurized vessel connected to the membrane on the filtrate side. The main parameters to take into account are the rate of the aqueous phase and the pressure of the organic phase through the pores. When the aqueous phase rate increases, the nanoparticle size and the organic phase flux slightly decreases. Moreover, the organic phase pressure has a great impact on the organic phase flux but no influence on the nanoparticle size (Charcosset & Fessi, 2005).

The membrane contactor technique has the advantage of producing both nanocapsules and nanospheres and controlling the size of nanoparticles by modifying the membrane. (Charcosset & Fessi, 2005). The membrane contactor technique has been used to produce vitamin E loaded nanoparticles prepared with polycaprolactone scaled up to 8-fold larger than the laboratory scale, obtaining a single batch size of 600 mL. From laboratory-scale to pilot-scale was reported a decrease in particle size and the encapsulations efficiency remained high (Khayata et al., 2012).

Although the methods for nanoparticle production for flash nanoprecipitation and membrane contactor showed feasibility to scale-up, there is a lack of information in the literature about the methods' practicality and implementation.

2.5 Comparison of scale-up devices

Polymeric nanoparticles have been recognized as promising delivery systems (Galindo-Rodríguez et al., 2005). This review shows some of the devices able to produce nanoparticles at a scalable level by solvent displacement. Table 2.1. compiles the main differences between the methods previously reported.

Table 2.1. Comparison of the three scale-up methods

T-mixer	Flash nanoprecipitation devices	Membrane contactor
Provides appropriate mixing of the phases (Briançon et al., 1999).	Impinging jets creates supersaturation producing a homogeneous solution (Chow et al., 2015).	Uses a filtration device to produce nanoparticles. Complex set-up.
Device with a simple design.	Zein NPs were successfully produced in a CIJM by Wan et al. (2015).	Scaled up to 8 -fold the lab-scale (Khayata et al., 2012).
Production in a facile and reproducible way (Galindo-Rodriguez et al., 2005).	Limitation: In CIJM the NPs solution showed low stability and aggregation (Chow et al., 2015).	Particles' size decreased from lab to pilot-scale (Khayata et al., 2012).
Continuous feeding process, thus continuous production of NPs (Vauthier & Bouchemal, 2009).	MIVM is composed by 4 inlets: each can be loaded with solvents at different ratios, materials and flow rates (Tao et al., 2019).	Encapsulation efficiency remained high (Khayata et al., 2012).
NPs batches up to 20-fold larger than lab-scale (Vauthier & Bouchemal, 2009).	MIVM allows better control of particle size than CIJM (D'Addio & Prud'homme, 2011).	Size of NPs is controlled by modifying the membrane (Charcosset & Fessi, 2005).
Adjusting flow rate of the phases allows production of batches with different volumes (Galindo-Rodriguez et al., 2005).	Both devices can be operated in parallel with several units scaled-up (Tao et al., 2019).	Vitamin E loaded NPs were successfully produced in a pilot-scale set-up (Khayata et al., 2012).
Limitation: low polymer concentration, otherwise polymer precipitates (Briançon et al., 1999).	Good reproducibility (Tao et al., 2019).	Limitation: Of the three methods, membrane contactor showed lower batch volume production.

CHAPTER 3 PRODUCTION AND CHARACTERIZATION OF FOOD GRADE NANOPARTICLES AT LABORATORY-SCALE

3.1 MATERIALS AND METHODS

3.1.1 Nanoparticle production

3.1.1.1. Materials

Ethylcellulose polymer with a viscosity ranged between 40 to 52 cP, molecular weight 160.0 g/mol and ethoxyl content of 48 to 49.5% was obtained from Ashland (Wilmington, DE, USA) in the powder form with product number 44331. Zein (product number Z3625) and β-carotene (>97% UV, lot number BCBR8106V) with molecular weight 536.87 g/mol were purchased from Sigma Aldrich (Saint Louis, MO, USA). β-carotene was kept at -22 °C and in darkness until use. All samples containing β-carotene during the experiments were protected from light. Ethanol absolute (99.8% purity, molecular weight 46 g/mol) was obtained from Honeywell Riedel-de-Haën (Muskegon, MI, USA). Pure water was obtained by a Milli-Q system (Milipore).

3.1.1.2. Production of ethylcellulose nanoparticles

The development of ethylcellulose nanoparticles was based on the methodology described by Fessi based on the interfacial polymer deposition following solvent displacement (Briancon, et al., 1999). Briefly, EC were dissolved in ethanol during at least 4 h at room temperature. Afterwards, water (5 mL at a time) was injected into the organic phase with continuous stirring (240 rpm using a magnetic stirrer) at room temperature. The solution was kept stirring for 15 min. An experimental design (Table A.1, ANNEX A) was used to evaluate different conditions (EC concentration and antisolvent concentration) in the size and polydispersity index of the nanoparticles. The optimal formulations were chosen based on the size by intensity and polydispersity index of the nanoparticles.

To produce β-carotene loaded EC nanoparticles, several concentrations of β-carotene were tested based on its maximum solubility in ethanol. All formulations tested are presented in Table A.2 (ANNEX A). The organic phase was prepared by dissolving EC and BC in ethanol and then the same methodology used for the production of blank EC nanoparticles production.

After the production of nanoparticles, the solvent was evaporated using a rotary evaporator (IKA®-Werke GmbH & CO. KG, Germany) at 60 °C, under reduced pressure of at least 30 mbar until there was no ethanol left. The final volume was expected to be 40 mL, if water started to evaporate, the final volume was adjusted with more water.

In some characterization tests (i.e. FTIR and X-Ray Diffraction) the samples needed to be dried before the analysis. For that, the solution of nanoparticles without ethanol was frozen over night at -22 °C. Then, they were transferred to a freezer at -80 °C for at least 4 h and then freeze-dried using a Freeze Dryer (Lyoquest -55 °C Plus Eco, Telstar, Spain) for 3 days to get a solid powder of nanoparticles.

3.1.1.3. Production of zein nanoparticle

Zein nanoparticle's preparation was also based on the methodology described by Fessi. Blank zein nanoparticles were firstly prepared to determine the optimal formulations (Briançon et al., 1999). The experimental design used is presented in ANNEX A Table A.3. Three different conditions were tested, namely zein concentration, antisolvent percentage and the flow rate in which the organic phase was dropped into the aqueous phase. The formulations chosen were 0.4% zein, 90% antisolvent (water) concentration and flow rate 0.7 mL/min based on the size by intensity and polydispersity index.

Briefly, 0.4% (0.4 g in 100 mL) of zein was prepared in ethanol solution (75%, v/v) making the organic phase. This solution was then added to the aqueous phase (water) in an amount sufficient for the final proportion of ethanol to be 10%. Therefore, for a total volume of 50 mL, the volume of zein solution added was 6.67 mL and the corresponding amount of water was 43.33 mL. The addition of the organic phase to the aqueous phase was controlled by a syringe pump (NE-1000 Programmable Single Syringe Pump, New Era Pump Systems Inc., USA) with a 12 mL Luer lock syringe (Soft-Ject®, Henk Sass Wolf, Germany) and a 15.80 mm diameter steel needle at a constant flow rate of 0.7 mL/min. The zein solution was added dropwise to the water at a constant stirring of 235 rpm using a magnetic stirrer and at room temperature. The final nanoparticle solution was maintained stirring for 15 min. The same methodology was used for the different concentrations of zein.

For the production of β-carotene loaded zein nanoparticles, a variety of BC concentrations were tested starting on its maximum solubility in ethanol. The formulations assayed are presented in

ANNEX A Table A.4. After testing several concentrations, the final concentration was 0.001% BC chosen based on the size by intensity and polydispersity index.

Because BC does not dissolve in aqueous ethanol, two different solutions were made for the preparation of the organic phase: i) 0.5 g of zein was dissolved in 100 mL of 75% aqueous ethanol solution and ii) 0.0025 g of BC was dissolved in 50 mL of 100% ethanol (0.005% BC concentrated solution). The two solutions were mixed by adding 10 mL of the BC solution to 40 mL of zein solution under constant stirring of 200 rpm thus making the final organic phase. Then, 6.25 mL of the latest solution was added dropwise to 43.75 mL of water, following the procedure described above.

An evaporation process was followed to remove ethanol by a rotary evaporator under the temperature 60 °C and reduce pressure of at least 40 mbar until all ethanol evaporated. In case of water evaporated, the volume would be adjusted to the expected volume of 45 mL. A freeze-drying step was also used when needed following the same procedure presented for ethylcellulose nanoparticles.

3.1.2 Nanoparticle characterization

3.1.2.1. Dynamic Light Scattering analysis

Parameters such as the mean size of the particles by intensity and by number, polydispersity index (PDI) and zeta potential were determined using dynamic light scattering (Nano Partica SZ-100, HORIBA, Japan). A disposable cuvette (ThermoFisher Scientific) and a carbon zeta potential cuvette were used for the measurements. All measurements were performed at 25 °C.

For each sample 5 measurements were performed, each with a duration of 180 seconds and using a detection angle of 90°. For the zeta potential determination were performed 3 measurements for 90 seconds each.

3.1.2.2. Encapsulation Efficiency

The encapsulation efficiency was determined to assess the percentage of β-carotene that was successfully entrapped into the nanoparticles. Therefore, freshly produced nanoparticles were submitted to ultracentrifugation for the separation of nanoparticles from free non-encapsulated β-

carotene. The separation was achieved using an Ultracentrifuge (OPTIMA XE-100, Beckman Coulter Life Sciences, USA) with a type 70 Ti Fixed-Angle Titanium Rotor. Briefly, approximately 26 mL of nanoparticle solution was poured into a polycarbonate bottle and were centrifuged at 50 000 rpm, for 1 h. After the centrifugation, there was a visible solid pellet containing the nanoparticles with the encapsulated BC for both zein NPs and EC NPs and the free BC would be dispersed in the supernatant.

The BC dispersed in the supernatant was analyzed spectrophotometrically in a Microtiter plate reader (Synergy H1, BioTek Instruments, USA). 200 μL of supernatant was put in triplicate in a 96 well plate (ThermoFisher Scientific Inc., USA) as well as a blank solution of pure ethanol and measured at 453 nm, which corresponds to the maximum absorbance of BC. The concentration of free BC was estimated by a previously made calibration curve. All dilutions, concentrations and respective absorbances measured for the curve are present in Table B.1 and Figure B.1 (ANNEX B).

The encapsulation efficiency for both EC nanoparticles and zein nanoparticles was calculated by the following equation:

$$EE\ (\%) = \frac{A - B}{A} \times 100 \qquad \text{Eq 3.1.}$$

being, EE (%) the percentage of encapsulation efficiency, A the initial concentration of β-carotene in the suspension of particles, B the concentration of β-carotene in suspension after centrifugation.

3.1.2.3. Transmission electron microscopy

Parameters such morphology, particle size distributions and aggregation were analyzed through a transmission electron microscope (JEM-2100, JEOL Ltd., Japan) operating at 200 kV accelerating voltage. TEM micrographs were analyzed using the public domain software ImageJ. A drop of the sample solution (≈ 10 μl) was placed on a grid (ultra-thin carbon film on Lacey carbon support film, 400 mesh, Copper, Ted Pella Inc., USA). Then, contrast solution UranyLess EM Stain (Electron Microscopy Sciences (EMS), USA) was dropped on parafilm and the grid was placed on top of the drop so it could be stained. It was left to dry for approximately 5 hours at room temperature.

3.1.2.4. Fourier transform infrared (FTIR)

Measurements were made using a FTIR VERTEX 80/80v spectrometer (Bruker Corporation, MA, USA) in Attenuated Total Reflectance mode (ATR) with a platinum crystal accessory in the wavelength range: 4000—400 cm^{-1}, using 32 scans at a resolution of 4 cm^{-1}. All data is presented in transmittance percentage after a normalization to the maximum transmittance value.

The samples analyzed were empty and loaded zein and EC nanoparticles, and BC, zein and EC powder. All nanoparticle's samples were freeze-dried before the measurements.

3.1.2.5. X-Ray Diffraction

An X-ray diffractometer was used to evaluate the crystallographic structure of the samples through their diffraction pattern. Measurements were made using an X-ray diffraction system (X'Pert Pro MRD, Malvern Panalytical Ltd, UK). PANanalytical X'Pert HighScore Plus was the software used to gather data and analyse peak diffractions. Background noise was also measured. The powder sample was added to the glass slide through an adhesive glue and put on the sample holder for detection. The XRD diffractograms were acquired at room temperature, angular scans from 5° to 50° (2θ) were performed with a Cu source, X-ray tube (λ = 1.54056 Å) at 45 kV and 40 mÅ. The fine calibration offset for 2θ = −0.0372°.

The samples analyzed were empty and loaded zein and EC nanoparticles, and BC, zein and EC powder. The nanoparticles were freeze-dried before the measurements.

3.1.3 *In vitro* gastrointestinal digestion

An *in vitro* simulated digestion was performed to study the bioaccesibility of β-carotene entrapped in the polymeric nanoparticles made of ethylcellulose or zein, following the standardized static *in vitro* digestion protocol – an international consensus established by the COST Infogest network (Brodkorb et al., 2019a). In the protocol the sample is subjected to sequential oral, gastric and intestinal digestion using parameters of digestion (electrolytes, enzymes, bile, dilution, pH and time of digestion) based on available physiological data. The protocol can be divided into three phases: a preparation phase where enzyme activities and bile concentrations are assessed and stock solutions of simulated fluids are prepared, a digestion phase which exposes the food to oral, gastric and intestinal conditions; and the last phase is the sample preparation and treatment for

subsequent analysis (Brodkorb et al., 2019a).

3.1.3.1. PHASE 1 - Enzyme activities, bile concentration and stock solutions

The digestion involves the action of enzymes such as amylase, pepsin, lipase, trypsin and chymotrypsin. These enzymes need to be added in a specific amount (U/mL) defined in the protocol, therefore their activities must be accurately determined. This way, the pepsin activity and trypsin activity in pancreatin were determined to calculate the amount (mg/mL) of each, needed in the *in vitro* digestion. Amylase was not used since there was no starch present in the digested sample. The addition of gastric lipase was omitted due to the limited access of the commercially available enzyme.

Enzyme activity assays

Materials

Pepsin from porcine gastric mucosa was obtained from Sigma-Aldrich (St Louis, MO, USA) in powder form (product number P7012) was stored at -20 °C. Hemoglobin from bovine blood was purchased from Sigma-Aldrich (St Louis, MO, USA) with product number H2625, stored at 4 °C. Trichloroacetic acid with molecular weight 163.69 g/mol (product number T6399) was obtained from Sigma-Aldrich (Germany) and stored at 4 °C. Sodium chloride with molecular weight 58.44 g/mol and product number S1639 was obtained from Sigma-Aldrich (St Louis, MO, USA).

Pancreatin from porcine pancreas (product number P7545), TAME (Nα-p-Tosyl-L-arginine methyl ester hydrochloride, product number T4626) and calcium chloride (product number C3306, molecular weight 110.89 g/mol) were purchased from Sigma-Aldrich (St Louis, MO, USA).

Trizma base from Sigma-Aldrich (St Louis, MO, USA) with product number T1503. Hydrochloric acid purchased from ThermoFisher Scientific with molecular weight 36.46 g/mol. Pure water was obtained from a Milli-Q system (Milipore).

Pepsin activity assay

Pepsin activity assay is based on the spectrophotometric stop reaction method. The principle of the assay is that hemoglobin diluted in water in the presence of pepsin produces TCA-soluble

tyrosine peptides. One unit will produce a ΔAbs_{280} of 0.001 per minute measured at TCA-soluble products (pH 2 and 37°C) (Brodkorb et al., 2019, supplementary information). Two different solutions were prepared previously to the assay: substrate and enzyme solutions.

Hemoglobin was used as substrate dissolving 0.5 g of 25 mL of water and adjusting the pH to 2 with 0.3M HCl. To prepare the enzyme solution firstly 88 mg NaCl plus 12 mg Trizma base were dispersed in 10 mL water and the pH adjusted to 6.5 with 0.3M HCl. Then, 10 mg of pepsin were dissolved in the previous solution to obtain a final concentration of 1 mg/mL of pepsin.

For the assay, pepsin was diluted to prepare 6 different concentrations: 5, 10, 15, 20, 25, 30 μg/mL. 500 μL of substrate solution was pipetted into 2 mL Eppendorf tubes and incubated for 4 minutes at 37 °C and 300 rpm in a ThermoMixer® C (Eppendorf). 100 μL of each pepsin concentration was added and incubated for 10 min exactly. After that time, 1 mL of 5% (w/v) TCA solution was added to stop the reaction. For each enzyme concentration, a blank sample was prepared the same way, but pepsin was added after the addition of TCA, which stops the reaction. All tubes were then centrifuged to precipitate the remaining hemoglobin for 30 minutes at 6000x *g*. The supernatant was put on disposable cuvettes (BRAND®, Germany) and the absorbance was read at 280 nm in a nanodrop (NanoDrop 3300, Fisher Scientific, Lda.).

The activity of pepsin (U/mg) was calculated by equation 3.2:

$$\text{Units/mg} = \frac{(\text{Abs Test} - \text{Abs Blank}) \times 1000}{\Delta t \times m \times 0.001} \qquad \text{Eq 3.2.}$$

Being Δt the duration of reaction in minutes (10 min), m the amount of pepsin (μg) in 1 mL of assay solution, 0.001 is the ΔAbs_{280} per unit of pepsin and 1000 the factor to convert μg to mg.

Trypsin from pancreatin activity assay

To measure the trypsin activity in pancreatin the kinetic spectrophotometric rate determination method was used. The principle is that TAME diluted in water in the presence of trypsin produces p-toluene-sulfonyl-L-arginine and methanol. One unit corresponds to the hydrolysis of 1 μmol of TAME per minute (pH 8.1 and 25 °C) (Brodkorb et al., 2019, supplementary information).

Substrate solution was prepared by dissolving 19 mg of TAME in 5 mL of water. The enzyme solution was prepared by dissolving 10 mg of pancreatin in 10 mL of 1 mM HCl resulting in 1 mg/mL concentration. Two dilutions were made: 0.5 mg/mL and 0.1 mg/mL. An assay solution

was also prepared by dissolving 51 mg of $CaCl_2$ and 223 mg Trizma base in 40 mL of water adjusting the pH to 8.1.

For the assay, 2.6 mL of assay solution and 0.3 mL of substrate solution were pipetted into disposable cuvettes (BRAND®, Germany) and put in the nanodrop for 3 minutes at 25 °C while being mixed with a magnetic stirrer. Then 100 μL of pancreatin solution was pipetted into the cuvette and the absorbance at 247 nm was measured each 30 seconds for 10 min. For the blank, the same procedure was followed adding 100 μL of assay solution instead of enzyme solution. The slopes ΔA247 [unit absorbance/minute] were calculated for both the blank and the test reactions by using the maximum linear rate over at least 5 minutes. The trypsin activity was calculated by the equation 3.3:

$$\text{Units/mg} = \frac{(\Delta\text{Abs Test} - \Delta\text{Abs Blank}) \times 1000 \times 3}{540 \times m} \qquad \text{Eq 3.3.}$$

Being ΔAbs Test and ΔAbs Blank the slope of the initial portion of the curve [unit absorbance/minute] for the enzyme and blank (without enzyme), respectively, 540 is the molar extinction coefficient (L/(mol · cm) of TAME at 247 nm, m is the amount (mg) of pancreatin in the final reaction volume and 3 is the total volume of the reaction mix, in mL.

Bile concentration assay

Materials

Bile bovine was purchased from Sigma-Aldrich (St Louis, MO, USA) in powder form with product number B3883. The concentration of bile acids in bile were measured with a commercial assay kit also obtained from Sigma-Aldrich (St Louis, MO, USA), catalog number MAK309. The bile acid kit assay contains several pre-made solutions: an assay buffer (cat. no. MAK309A), NAD solution (cat.no. MAK309B), probe (cat.no. MAK309C), Enzyme A (cat.no. MAK309D), Enzyme B (cat.no. MAK309E) and standard solution (cat.no. MAK309F).

Method

Bile acids concentration was measured following the supplier's protocol which provides a fluorometric method to measure the total bile acids. Firstly, a bile solution (60 mg/mL) was prepared with water. Dilutions were made to achieve three different final concentrations to be analyzed: 0.06 mg/mL, 0.03 mg/mL and 0.01 mg/mL. Three more stock solutions were

prepared:

- Internal standard reagent: 20 μL of standard solution + 230 μL water;

- Working reagent: 75 μL assay buffer + 8 μL NAD solution + 4 μL probe + 1 μL enzyme A + 1 μL enzyme B;

- Blank reagent: 75 μL assay buffer + 8 μL NAD solution + 4 μL probe + 1 μL enzyme B.

All samples were prepared in a 96 well opaque black plate and run in duplicate. Three different wells were prepared for each sample: sample, sample blank and internal standard.

20 μL of sample (different concentrations) were pipetted into the respective wells. 5 μL of water was pipetted into the sample and sample blank wells and 5 μL of internal standard reagent was pipetted into the internal standard wells. Then, 80 μL of working reagent was added to the sample and internal standard wells and 80 μL of blank reagent was added to the sample blank wells. The plate was then incubated for 20 minutes in the dark and the fluorescence intensity was read at λ_{ex}=530 nm and λ_{em}=585 nm.

The bile concentration was calculated using the equation 3.4:

$$[\text{Bile acids}] = \frac{A - B}{C - A} \times 20 \times n \qquad \text{Eq 3.4.}$$

Being A the fluorescence intensity values of sample, B the fluorescence intensity values of sample blanks and C the fluorescence intensity values of internal standard; 20 μM is the concentration of the internal standard and n is the dilution factor. Final bile acids concentration is given in μM.

Simulated digestion fluids preparation

The stock electrolytic solutions were prepared according to the INFOGEST static *in vitro* simulation of gastrointestinal digestion protocol (Brodkorb et al., 2019a), as shown in the Table 3.1. SSF, SGF and SIF were prepared 1.25 times concentrated, considering the later dilution (4:1) with enzymes and $CaCl_2(H_2O)_2$ added in the day of use to avoid precipitation.

Table 3.1. Chemical composition of simulated salivary fluid (SSF), simulated gastric fluid (SGF) and simulated intestinal fluid (SIF) prepared from the stock solutions

Reagent	Stock solution		SSF (pH 7)		SGF (pH 3)		SIF (pH 7)	
	g/L	mol/L	mL	mmol/L	mL	mmol/L	mL	mmol/L
KCl	37.3	0.5	15.1	15.1	6.9	6.9	6.8	6.8
KH_2PO_4	68	0.5	3.7	3.7	0.9	0.9	0.8	0.8
$NaHCO_3$	84	1	6.8	13.6	12.5	25	42.5	85
NaCl	117	2	-	-	11.8	47.2	9.6	38.4
$MgCl_2(H_2O)_6$	30.5	0.15	0.5	0.15	0.4	0.12	1.1	0.33
$(NH_4)_2CO_3$	48	0.5	0.06	0.06	0.5	0.5	-	-
$CaCl_2(H_2O)_2$	44.1	0.3		1.5		0.15		0.6
HCl	-	6	0.09	1.1	13	15.6	0.7	8.4

Salt solutions added to prepare the stock simulated solutions were made with the following reagents: KCl (product no. P9333), $NaHCO_3$ (product no.S5761), NaCl (product no. S1679), $MgCl_2(H_2O)_6$ (product no. M2670), $(NH_4)_2CO_3$ (product no. 68392) and $CaCl_2(H_2O)_2$ (product no. C3306) all purchased from Sigma-Aldrich (USA) and KH_2PO4 (product no. 121509) was purchased from PanReac AppliChem (Spain).

3.1.3.2. PHASE 2 – Digestion procedure

Four different samples were submitted to the digestion procedure: ethylcellulose nanoparticles loaded with β-carotene, zein nanoparticles loaded with β-carotene, free β-carotene dispersed in 100% sunflower oil (Fula, Portugal) and the blank using water. All samples containing β-carotene were prepared in order to achieve a concentration of [BC] = 20 μg/mL. Nanoparticle's solutions were concentrated in the rotary evaporator. All samples were digested in triplicate.

In this study, the digestion was evaluated at two time points: after the gastric phase and after the intestinal phase.

Oral phase

In the oral phase the sample was diluted 1:1 (v/v) with simulated salivary fluid, calcium chloride and water.

Briefly, to 5 mL of each sample, 4 mL of SSF, 25 μL $CaCl_2(H_2O)_2$ 0.3 M and 0.975 mL of water were added. The tubes were incubated in an orbital incubator (Fisher Scientific) for 2 minutes at 37 °C and 150 rpm.

Gastric phase

For the gastric phase, a pepsin solution 13.84 mg/mL (2000 U/mL) in water was prepared based on the activity previously determined (ANNEX C).

The 10 mL of oral bolus obtained in the former phase were diluted 1:1 (v/v) with 8 mL of SGF, 1 mL of pepsin solution (to achieve an activity of 2000 U/mL in the final digestion mixture), 5 μL $CaCl_2(H_2O)_2$ 0.3, 300 μL HCl 1 M and 695 μL of water. The pH was adjusted to 3.0 using HCl.

The samples were incubated in an orbital incubator (Fisher Scientific) for 2 h at 37 °C and 150 rpm.

Intestinal phase

For the intestinal phase, bile solution 60 mg/mL and pancreatin 148.15 mg/mL (100 U/mL) were prepared in SIF based on the activity previously determined (ANNEX C).

The 20 mL of gastric chyme from gastric phase were diluted 1:1 (v/v) with 6.57 mL SIF, 5 mL of pancreatin solution (to achieve a trypsin activity of 100 U/mL in the final digestion mixture), 4.43 mL of bile (to achieve a concentration of 10 mM in the final mixture), 40 μL $CaCl_2(H_2O)_2$, 0.3 M, 140 μL HCl 1 M and 3.82 mL of water. The pH was adjusted to 7.0.

The samples were incubated in an orbital incubator (Fisher Scientific) for 2 h at 37 °C and 150 rpm.

3.1.3.3. PHASE 3 – Sample Analysis

For the sample analysis the digested tubes at both time points were centrifuged for 20 min at 4 °C and 3100 $\times g$. For the bioaccesibility analysis, β-carotene must be extracted from the digested

samples to be quantified. Besides the samples digested, β-carotene present in the non-digested samples (BC loaded EC nanoparticles and BC loaded zein nanoparticles) was also extracted.

Extraction of BC

BC extraction was performed by solvent-solvent extraction using organic solvents following the methodology reported by (Wright et al. (2008). After centrifugation, 500 μL of supernatant was transferred to a tube to begin the extraction. The organic solvents were added: 0.5, 3.0 and 1.0 mL of ethanol, acetone and distilled water, respectively, vortexing for 10 seconds between each addition. 2 mL of hexane was then added, the tubes were mixed by inversion and rested for 20 mi. The top organic layer was removed, and 1 mL of hexane was added again and removed after 5 minutes. This step was repeated twice. The final 5 mL of hexane pooled were evaporated (Modular Centrifugal Evaporator, Fisher Scientific, Lda.) at 40 °C under vacuum until approximately 500 μL was left. All volumes were set to 500 μL equally adding fresh hexane if needed and transferred to vials for posterior analysis.

For the non-digested BC loaded zein nanoparticles samples, an extra step was added to evaluate the extraction efficiency: the initial sample was diluted into 3 different β-carotene concentrations (10.0, 5.0 and 2.5 μg/mL) and the extraction was performed. Extraction efficiency was calculated using equation 3.5:

$$\text{Extraction efficiency (\%)} = \frac{C_E}{C_0} \times 100 \qquad \text{Eq 3.6.}$$

C_E being the concentration of β-carotene extracted and C_0 the initial β-carotene concentration.

Another test to disintegrate the zein proteins was evaluated. Two methods were applied: the use of DMSO (Dimethyl sulfoxide, product no. 276855, Sigma-Aldrich, USA) and alcalase (PJN04032, Novozymes, Denmark) diluted 20× in PBS (Phosphate-Buffered Saline, cat. no. AM9624, Thermo Fisher Scientific, Lithuania). Briefly, to 500 μL of sample, 1 mL of breakage solution was added and incubated for 10 min at 45 °C and 300 rpm. Then, the extraction by organic solvents was performed.

β-carotene quantification through HPLC

The β-carotene was quantified by high liquid performance chromatography (HPLC) using an Agilent 1260 Infinity Quaternary LC (Agilent Technologies, Santa Clara, USA) equipped with a Kinetex 2.6 μm XB-C18 column (150 x 4.6 mm, Phenomenex, USA). The mobile phase was composed of

Methanol and Acetonitrile (90:10) under a flow rate of 1.8 mL/min. The β-carotene was eluted and monitored at 450 nm, being the retention time of 4.2 min and the quantification limit of 0.156 mg/mL.

From the HPLC results, information was obtained about the concentration of the samples. Through the concentrations, the mass of BC was calculated given the digestion volume (20 mL or 40 mL for gastric or intestinal phase, respectively).

The bioaccessibility of encapsulated BC after digestion was calculated using the following equation:

$$\text{Bioaccessibility (\%)} = \frac{m_1}{m_2} \times 100 \qquad \text{Eq 3.6.}$$

Being m_1 the mass of BC in the micelle fraction after digestion and m_2 the initial mass of BC.

3.1.4 Statistical analysis

The data obtain from the experimental design were submitted to a statistical analysis using Statistica software (release 7, edition 2004, Statsoft, Tulsa, OK, USA). Pareto charts were drawn to express visually the statistical significance of each factor and the interactions between factors visually.

3.2 RESULTS AND DISCUSSION

Two different biopolymers were used to produce nanoparticles with similar size and polydispersity. For that purpose, the nanoprecipitation method was used and according to the biopolymer used, different conditions were evaluated. An experimental design was used for each type of biopolymer. For EC-based nanoparticles, the evaluated parameters were the effect of EC and antisolvent concentration being all the other parameters maintained constant. In the case of zein-based nanoparticles, the parameters evaluated were zein and antisolvent concentration and the organic phase addition rate.

For all the results shown in this section, the β–carotene concentration presented is always regarding the concentration in the organic phase before the production of the nanoparticles.

Results shown for the experimental design were optimized by statistical analysis. During the evaluation of the factors, the dependent variables were the size by intensity and the polydispersity index.

3.2.1 Ethylcellulose nanoparticles

The optimization of the production of EC nanoparticles has as independent variables the polymer concentration and antisolvent concentration. The assayed formulations and obtained values are presented in Table A.1 (ANNEX A).

Figures 3.1 and 3.2 shows the effects of varying antisolvent and polymer concentration on size by intensity and PDI, respectively. Polymer concentration varied between 0.1, 0.2 and 0.4% and antisolvent concentration varied between 60, 70 and 80% (v/v).

Results reveal that the parameters that influence the most the size of the EC nanoparticles are both EC concentration and antisolvent concentration with statistical significance ($p<0.05$) as can be seen in Figure 3.1 A). The aim was to obtain a size-controlled production of nanoparticles with a narrow size distribution. Therefore, the main parameters to take into account are the correlation of these two concentrations: lower sizes by intensity were a combination of lower ethylcellulose concentrations (0.1%) and higher antisolvent concentrations (80%) (Figure 3.1. B)). This phenomenon can be explained by the fact that increasing the polymer concentration will increase the viscosity of the organic phase, making it difficult to diffuse the solvent into the water, lowering the nucleation rate and producing bigger aggregates (Chow et al., 2015). Moreover, increasing the

antisolvent concentration will induce a faster solvent diffusion into the water and smaller particles are formed (Miladi et al., 2016).

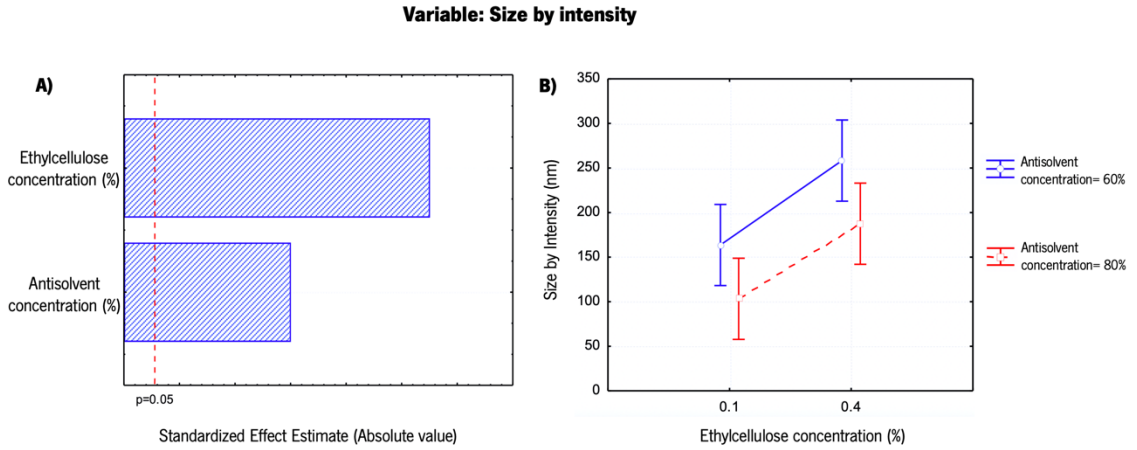

Figure 3.1. A) Pareto chart of standardized effects. B) Plot of marginal means and conf. limits (95%). Variable: Size by intensity.

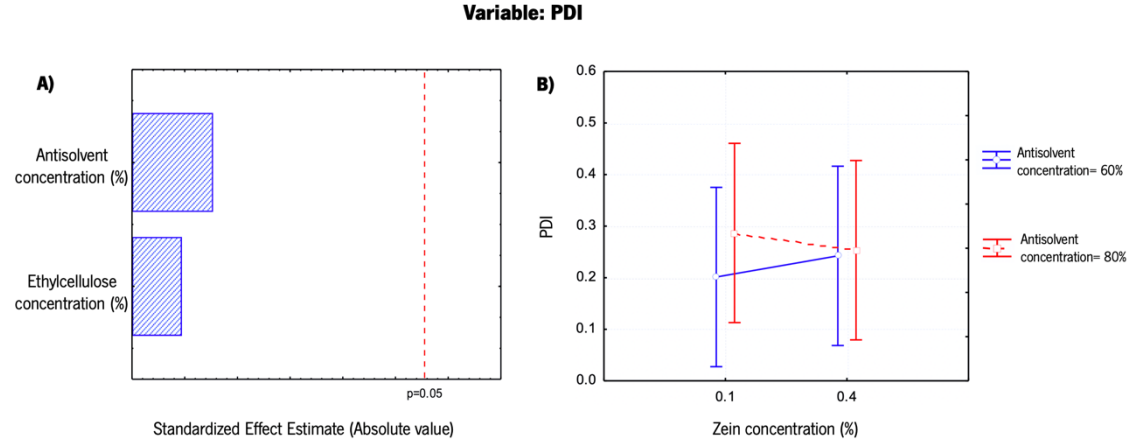

Figure 3.2. A) Pareto chart of standardized effects. B) Plot of marginal means and conf. limits (95%). Variable: PDI.

The formation of large particles will contribute to a wider particle distribution, that can explain why higher polymer concentration leads to slightly high PDI. However, none of the variables tested for ethylcellulose had a significant influence over the PDI ($p>0.05$) (see Figure3.2. A)). Polydispersity index measures the homogeneity of the dispersion of nanoparticles, PDI values greater than 0.5 can represent aggregation of particles (Ahmed et al., 2012). All measures performed stayed below this value. Since only the size by intensity was significantly affected by the conditions tested, the parameters were chosen based only on size by intensity.

3.2.2 Zein nanoparticles

The optimization of the production of zein nanoparticles has as independent variables the polymer concentration, antisolvent concentration and flow rate. The assayed formulations and obtained values are presented in Table A.3 (ANNEX A).

Figures 3.3 and 3.4 shows the effects of varying those variables on size by intensity and PDI, respectively. Polymer concentration varied between 0.4, 0.6 and 0.8%, antisolvent concentration varied between 80, 85 and 90% (v/v) and flow rate varied between 0.3 and 0.7 mL/min.

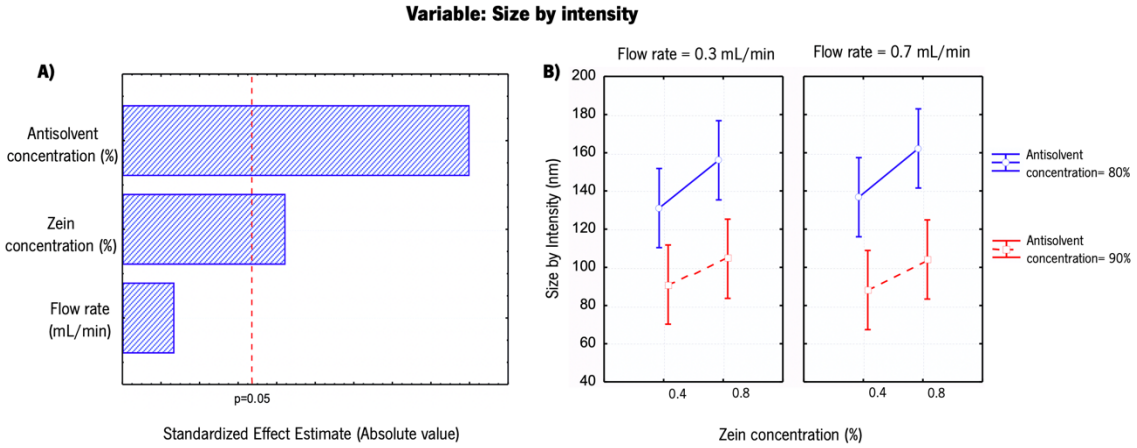

Figure 3.3. A) Pareto chart of standardized effects. B) Plot of marginal means and conf. limits (95%). Variable: Size by intensity.

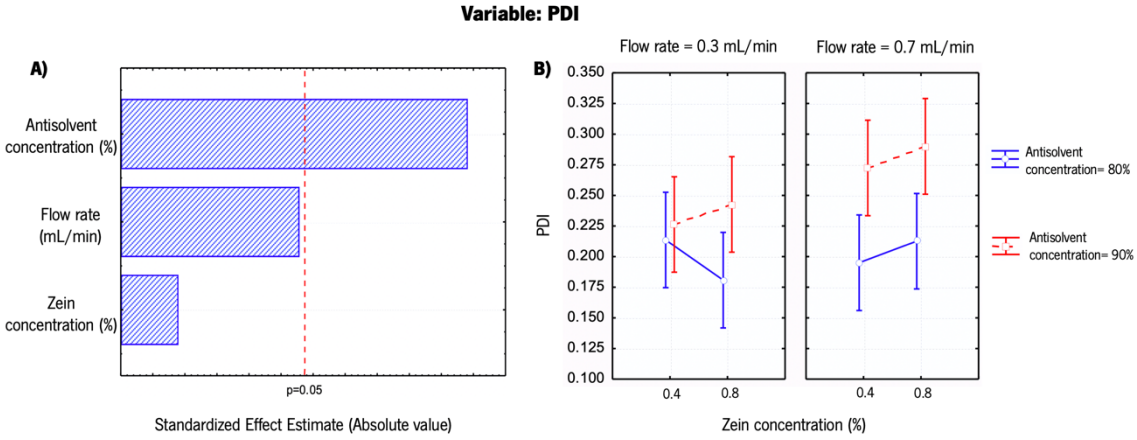

Figure 3.4. A) Pareto chart of standardized effects. B) Plot of marginal means and conf. limits (95%). Variable: PDI.

Results shown in Figure 3.3 A) reveal that the parameters that most influence the size by intensity are mostly the antisolvent concentration and zein concentration with statistical significance ($p<0.05$). In Figure 3.3 B) it can be seen how these parameters influence the particles: higher concentrations of antisolvent shows a significant drop on the size by intensity, e.g., for a 0.7 mL/min flow rate and 0.4% zein concentration values of size goes from approximately 140 to 90 nm, when the antisolvent concentration goes from 80% to 90%. Lower concentrations of zein also revealed the smaller nanoparticles' sizes. These results are similar to the ones for ethylcellulose nanoparticles and can be explained by the same phenomenon: lower polymer concentration and higher amounts of antisolvent lowers the viscosity of the suspension inducing fast miscibility of phases and smaller particles formed. Also, when less zein and more water is used, it results in less accessible zein polymer in suspension that forms nanoparticles, thus decreasing the agglomeration of particles as well as its size (Xu, Jiang, Reddy, & Yang, 2011).

Li et al. (2017) reported similar results, increasing the zein concentration also resulted in increased particle size and PDI.

For the polydispersity index, significant statistical differences were found for the antisolvent concentration ($p<0.05$). However, in Figure 3.4 B), it can be seen that the antisolvent concentration has an opposite effect of what would be expected, i.e., in this case, the higher amount of antisolvent resulted in higher PDI, varying from 0.275 to 0.200, for flow rate 0.7 mL/min and 0.4% zein concentration. Nevertheless, the PDI remained under the value of 0.5, which means good homogeneity.

Because the flow rate did not have a significant influence on both variables tested, 0.7 mL/min was chosen to produce the nanoparticles due to it being higher rate. The other conditions were chosen based on the results of its combination: higher antisolvent concentration (90%) with lower zein concentration (0.4%).

After the selection of the conditions to obtain the nanoparticles with small sizes and PDI values, was evaluated the encapsulation of β–carotene.

3.2.3 Encapsulation Efficiency

The encapsulation efficiency of nanoparticles was tested using different concentrations of β–carotene. One of the first aspects considered was the effect of BC in nanoparticles size and PDI,

and it was observed that the highest concentration that allowed to obtain nanoparticles with small sizes and PDI values was 0.0004% (Table A.2., ANNEX A) for EC and 0.001% (Table A.4., ANNEX A) for zein nanoparticles. Based on these BC concentrations limits, the EE was determined for these and lower concentrations of BC.

Once the encapsulation efficiency is determined by the amount of BC that remained free in the suspension, and therefore, was not encapsulated, higher encapsulation efficiencies may mean two different issues: i) low amount of BC used, not enough to attach to all polymer available that resulted in some polymer being empty, therefore no free BC remained in suspension; ii) the right amount of BC used that resulted in all the polymer being saturated with BC and therefore no free BC remained in suspension. Lower values of encapsulation efficiency are a cause of larger amounts of BC used that exceeded the saturation limit for the polymer available, leaving BC in solution.

Table 3.2 presents the EE of BC obtained for EC and zein nanoparticles. Results show that the use of higher concentrations of BC resulted in a decrease of the encapsulation efficiency for EC, but the opposite for zein nanoparticles.

Encapsulation efficiency curves typically reach a peak at a certain optimal BC concentration, and then drop into much lower values of encapsulation efficiencies. The preferred value for the encapsulation efficiency is the BC concentration value below the one where the encapsulation efficiency drops.

Table 3.2. Percentage of encapsulation efficiency on different formulations of ethylcellulose nanoparticles and zein nanoparticles varying the BC concentration

	BC Concentration (%)	Encapsulation efficiency (%)
Ethylcellulose nanoparticles	0.00004	85.75
	0.00008	78.63
	0.0004	66.56
Zein nanoparticles	0.0005	82.65
	0.001	92.69

During the production of BC loaded EC nanoparticles, some BC would precipitate on the surface of the dispersion. This phenomenon can be explained by the large amount of BC used. Because there is a saturation limit for the incorporation of free BC into the dissolved ethylcellulose polymer, the excess BC precipitates and is not be encapsulated. This hypothesis is supported by the observation that a precipitate is formed when higher BC concentrations are used (Hayden et al., 2018).

In the case of EC nanoparticles, 0.00004% is the concentration for which the maximum EE is obtained. It is important to mention that higher EE could be obtained if the concentrations of BC were lower. However, as one of the goals is to improve the bioaccessibility of BC, higher concentrations are needed, and therefore the concentration of BC 0.0004% was chosen to move forward.

For the zein nanoparticles, two concentrations were tested, being chosen a concentration of 0.001% of BC since it shows a greater value of encapsulation efficiency (92.69%). The EE for higher concentrations of BC was not evaluated due to the high PDI values (>0.5) obtained for the nanoparticles (Table A.4, ANNEX A).

In this case, to higher BC concentrations is observed an increase of the EE. This may mean that a higher amount of BC can be encapsulated (and the amount of zein used hasn't yet reach its saturation limit), however based on the effect of higher BC concentrations in the zein nanoparticles, the value obtained for the EE (92.69%) could be the maximum possible value without changing the size and PDI of the nanoparticles. Similar results were obtained by Wang et al. (2018). The encapsulation efficiency of BC loaded zein nanoparticles would reach its peak approximately at 50% of encapsulation efficiency and then slightly decrease if the concentration of BC was lowered, since there was no enough BC attaching to the zein.

3.2.4 Size, PDI and Zeta Potential

The size by intensity and number, PDI and zeta potential of the loaded nanoparticles was determined using the BC concentrations. The values obtained for blank EC nanoparticles and loaded EC nanoparticles were –60 ± 1.7 and –93.29 ± 2.6 mV, respectively, meaning that the samples showed good stability behavior. Blank zein nanoparticles and loaded zein nanoparticles presented values of +63.5 mV and +70.5 mV, respectively. The zeta potential can be an indicator

of how stable a suspension of nanoparticles is, i.e. higher absolute values indicate higher repulsion between particles, meaning that the suspension is stable. In general, zeta potential values outside the range +30 mV to –30 mV have high stability behavior (Trivedi et al., 2017). The zeta potential values obtained for unloaded and loaded NPs either for EC or zein are different (p<0.05).

Table 3.3. Size by intensity and number, PDI and zeta potential for ethylcellulose and zein nanoparticles with and without BC measured by DLS. (Data are expressed as the mean ± SD)

	Size by intensity (nm)	Size by number (nm)	PDI	Zeta potential (mV)
Blank EC NPs	69.4 ± 2.1 ab	49.1 ± 2.3 a	0.176 ± 0.038 a	–60.7 ± 1.7 a
0.0004% BC loaded EC NPs	59.9 ± 9.0 a	39.1 ± 8.5 b	0.274 ± 0.015 b	– 93.26 ± 2.6 b
Blank zein NPs	81.5 ± 7.3 bc	53.8 ± 4.4	0.341 ± 0.049 b	63.5 ± 1.6 c
0.001% BC loaded zein NPs	82.7 ± 8.1 c	62.4 ± 7.9	0.286 ± 0.058 b	70.5 ± 0.7 d

Values reported are the mean ± standard deviation (sd). Different letters (a–d) in the same column indicate a statistically significant difference (p<0.05).

Ethylcellulose nanoparticles shows a drop in the size by intensity, as well as number, when loaded with BC. Decreasing from 69.4 (± 2.1) to 59.9 (± 9.0) nm. However, the PDI shows higher values for the loaded particles, which may be due to the surface area variation that can occur as a result of BC addition. Zein nanoparticles showed similar results for blank and loaded nanoparticles, approximately 80 nm for the size by intensity. However, for the loaded nanoparticles, higher values were obtained for the number distribution and PDI values were lower. In general, all nanoparticles were below the size 100 nm and with PDI lower than 0.5.

3.2.5 Transmission electron microscopy

Morphological analysis was performed on the produced nanoparticles. Results are shown in Figure 3.5 and Figure 3.6. TEM images provides information from the nanoparticles' direct observation. Images are obtained through the interaction of a beam of electrons and the sample (with contrast solution previously added) (Reimer, 2013).

From the observation of Figure 3.5., all EC nanoparticles showed spherical shape, which was consistent with the results obtained by DLS. Nanoparticles' diameters were roughly similar. However, it can also be seen a broader range of particles, large amounts of smaller sizes (<100 nm) and a few of larger sizes (>100 nm), which confirms the number distributions obtained by DLS. For loaded BC ethylcellulose nanoparticles, aggregation seemed to occur, and it may lead to an increase of the PDI obtained by DLS.

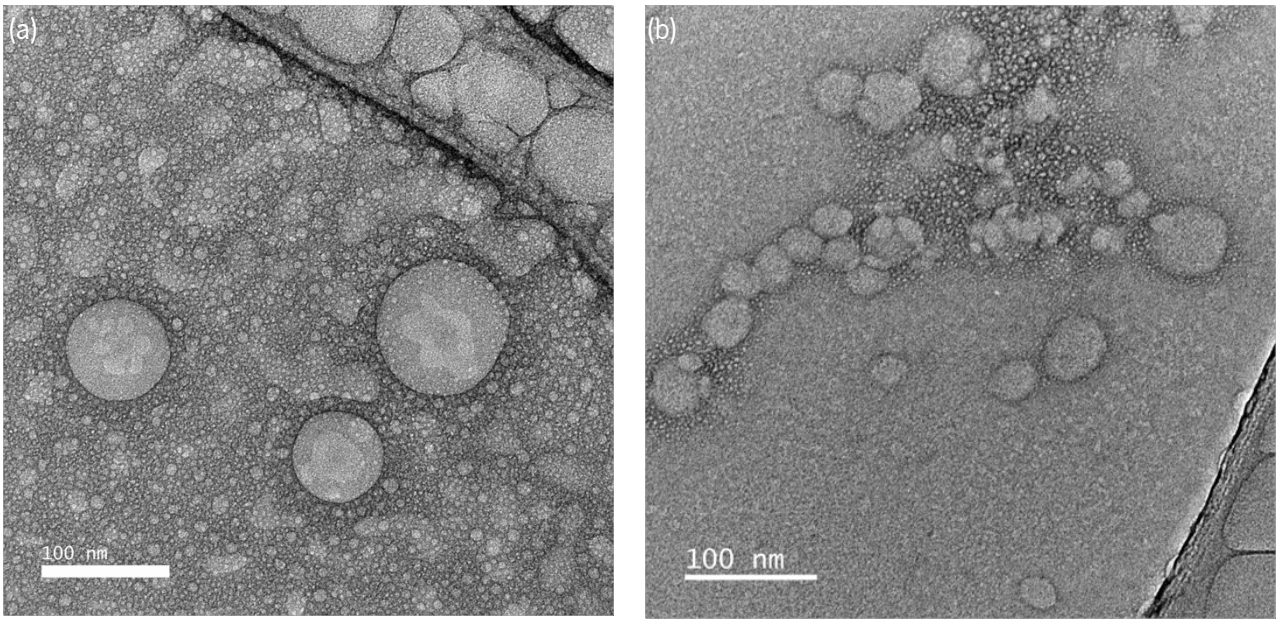

Figure 3.5. TEM images of blank EC nanoparticles (a) and BC loaded EC nanoparticles (b) at 100 000x.

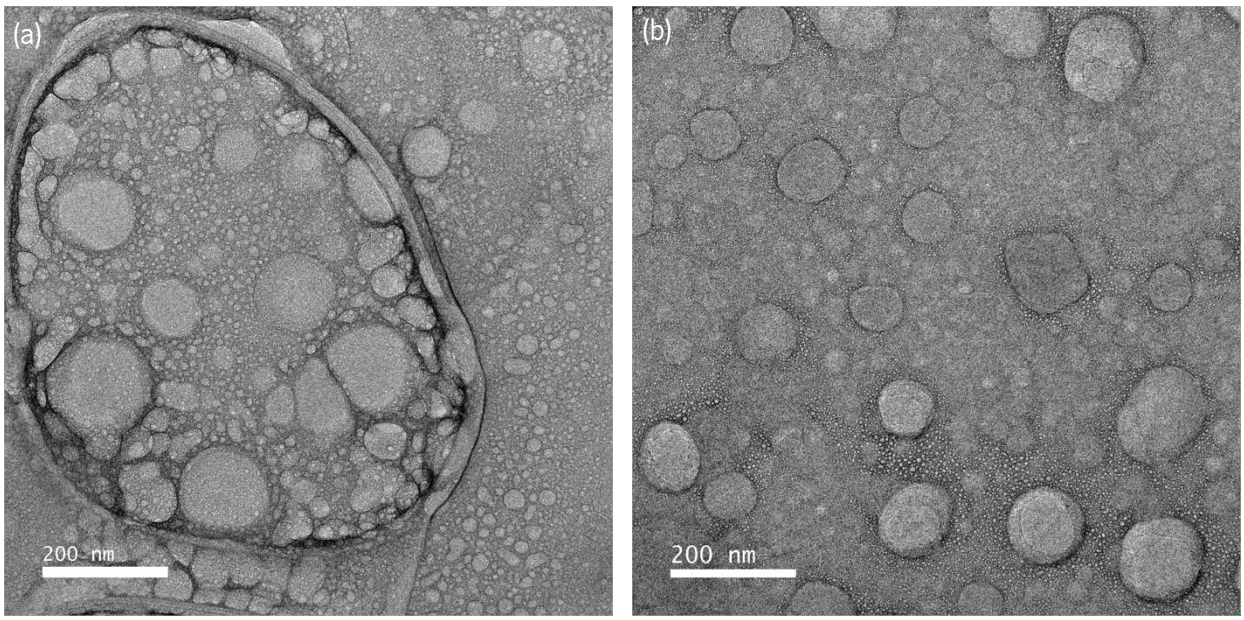

Figure 3.6. TEM images of blank zein nanoparticles (a) and beta-carotene loaded zein nanoparticles (b) at 50 000x.

Size measurements using dynamic light scattering yielded a size by intensity of about 80 nm which was compatible with the TEM image for zein nanoparticles. In addition, various-sized nanoparticles were present, which contributed for smaller number distributions. All particles had spherical shape. When comparing the blank nanoparticles with loaded nanoparticles it is important to mention that they remained without significant changes to the morphology of the particles.

3.2.6 Fourier Transform Infrared spectroscopy

Fourier transform infrared (FTIR) spectroscopy was used to determine the nanoparticles' chemical structure at molecular scale. Each molecule has a characteristic infrared spectrograph equivalent to a fingerprint, making it possible to identify the constituting elements and bonding arrangement of a sample. In addition, FTIR can be used to find the compatibility between drug and polymers (Baudot, Tan, & Kong, 2010).

Pure samples spectrum was used as a reference for evaluating their presence in the nanoparticle form. β-carotene spectra show a clear peak at 964 cm^{-1}, which is the trans conjugated alkene CH out of plane deformation mode (Yi et al., 2015).

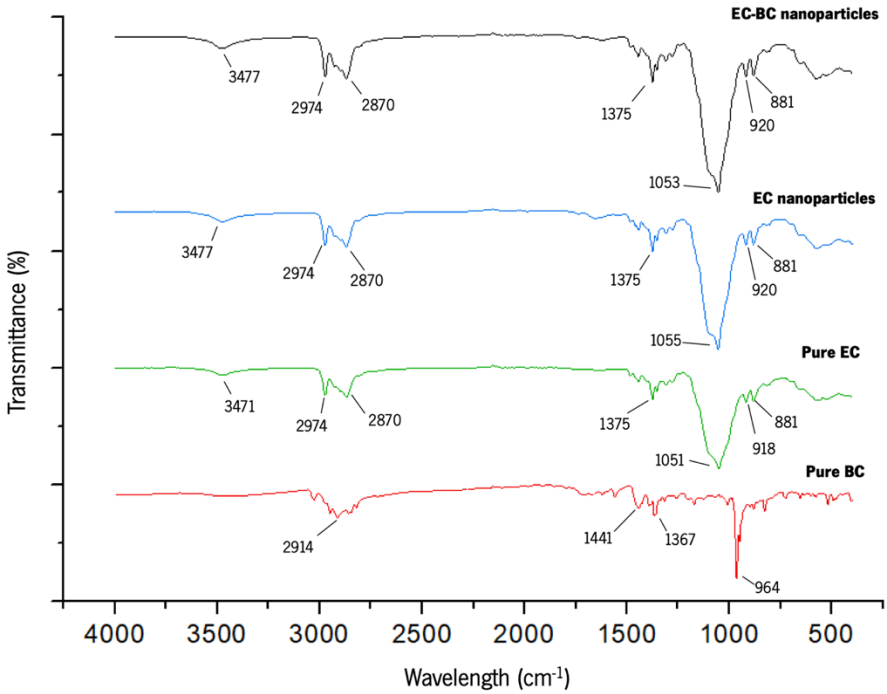

Figure 3.7. FTIR spectra of β-carotene powder, ethylcellulose powder, ethylcellulose nanoparticles and β-carotene loaded ethylcellulose nanoparticles.

The absorption characteristic peaks of ethylcellulose (Figure 3.7) at 1051 cm^{-1}corresponds to C—O—C stretching and the wavelengths 2870 cm^{-1} and 2974 cm^{-1}corresponded to C—H. The band at 3471 $cm^{-1}$is due to the hydroxyl (O—H) stretching vibrations (Guo & Gray, 1994; Madni et al., 2014). From pure EC to the nanoparticle form there was only a peak shift from 3471 cm^{-1} to 3477 cm^{-1} (difference greater than the resolution of 4 cm^{-1}). These results reveal no significant change on the structure of EC when nanoparticles are produced. Even as loaded BC nanoparticles, no significant BC peaks were found. This may be due to the small concentration of BC used compared to EC concentration, since the intensity of the peaks of FTIR spectra are proportional to the concentration of the sample.

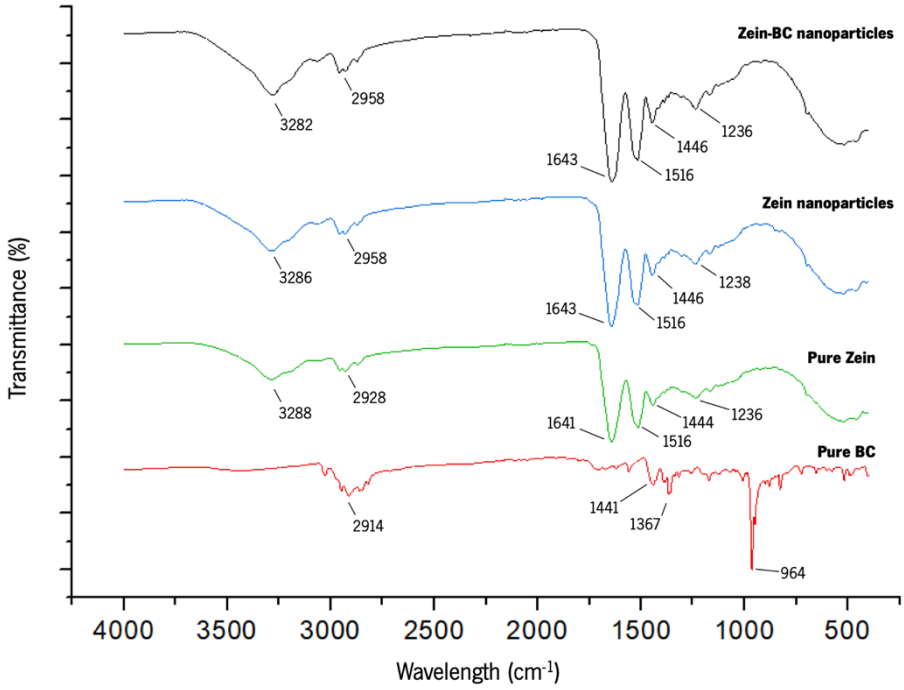

Figure 3.8. FTIR spectra of β-carotene powder, zein powder, zein nanoparticles and β-carotene loaded zein nanoparticles.

For pure zein, the characteristic bands of proteins can be seen in Figure 3.8. Protein bands that most stands out are amide I or C=O, usually in the range 1600-1700 cm^{-1}, stretching at 1641 cm^{-1} and amide II or N—H, usually present at 1500-1530 cm^{-1}, bending and stretching at 1516 cm^{-1}. Amide A or N—H is stretching at 3288 cm^{-1}; amide B or asymmetric stretching vibration of =C—H at 2928 cm^{-1}; and amide III or C—N stretching at 1236 cm^{-1}. Similar values can be seen in the encapsulation structures containing zein (Gómez-Mascaraque et al., 2017; Yi et al., 2015).

Amide A and amide III revealed different values for zein NPs and BC loaded zein NPs, however they were not significant due to the resolution being 4 cm^{-1}. Amide B showed a shift from 2928 to 2958 cm^{-1} when the material was in the form of nanoparticle. This implies that the formation of nanoparticles impacts the structure and conformation of the protein (Yi et al., 2015). In the loaded BC nanoparticles, there was no obvious difference in the amide bands, implying that the BC incorporated in the polymer may not show an obvious effect on the structural conformation of the proteins from the blank nanoparticles or that the concentration of BC used in the nanoparticles hampered the unequivocal identification of BC in the FTIR spectra of encapsulated particles (Gómez-Mascaraque et al., 2017).

3.2.7 X-ray diffraction

The X-ray diffraction (XRD) spectrum of a crystalline structure shows sharp peaks. Thus, the spectrum of the pure BC (Figure 3.9 and 3.10) showed that the compound is a crystalline material. However, the BC peaks were not visible in the loaded BC nanoparticles, either being EC or zein nanoparticles suggesting the BC is amorphous in both nano systems. Changes in BC crystallinity may be due to the precipitation without crystallization when in contact with the antisolvent in the nanoprecipitation procedure or during solvent evaporation (Yi et al., 2015).

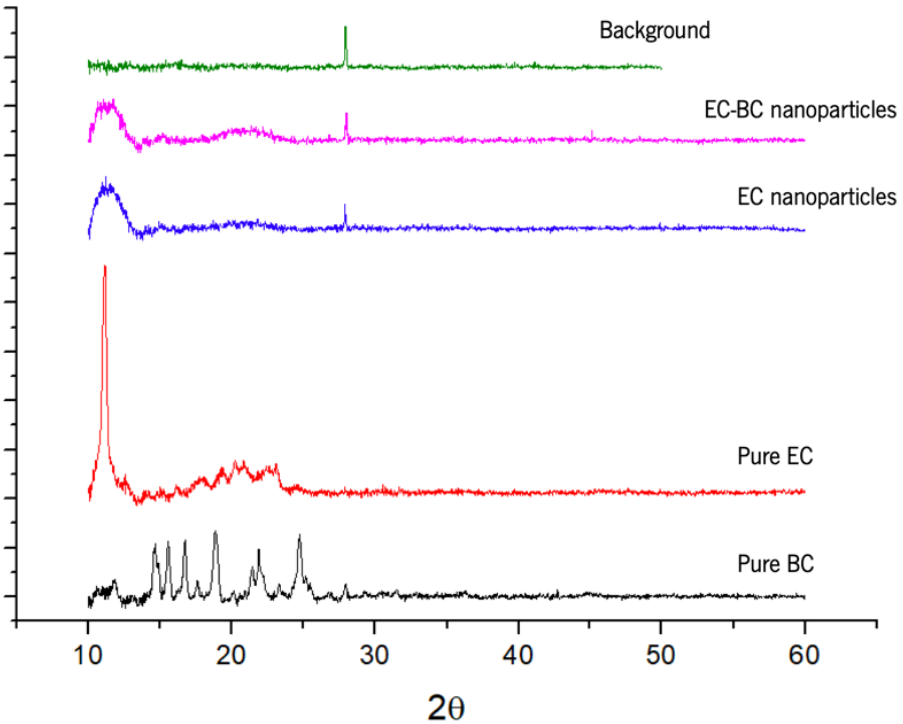

Figure 3.9. X-ray diffraction patterns of pure BC, pure EC, EC NPs, EC-BC NPs and background.

Pure EC spectra revealed sharp peaks, which confirmed the presence of crystalline structure (Khan et al., 2010). All nanoparticles' samples showed to be amorphous. However, EC characteristic peak showed an intensity able to be observed and can be also seen in EC nanoparticles and loaded EC nanoparticles.

Pure zein spectra did not show sharp peaks, instead it shows two humps, indicating the amorphous structure of the protein. A peak can be observed, however as it matches the background peak, it was not considered. Zein nanoparticles and loaded nanoparticles show similar amorphous spectra.

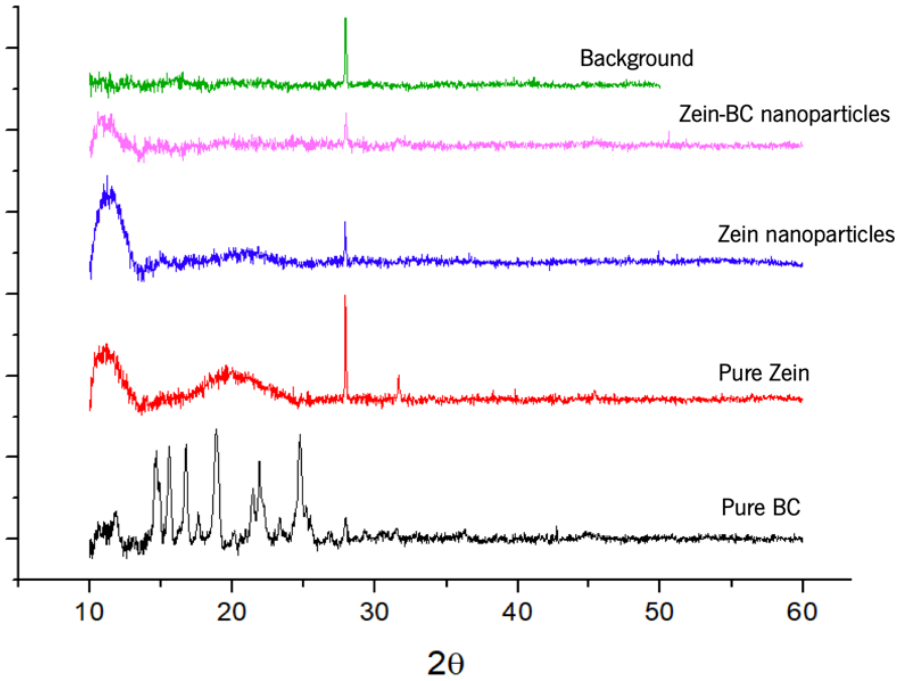

Figure 3.10. X-ray diffraction patterns of pure BC, pure zein, zein NPs, zein-BC NPs and background.

Results reported by Tao et al. (2019) revealed that nanoparticles produced by nanoprecipitation were usually amorphous and less stable during storage compared to their crystalline counterpart. Since amorphous compounds easily recrystallize in water therefore increasing aggregation, a solution desirable is a freeze-drying step to improve their stability.

3.2.8 *In vitro* digestion

The determination of the bioaccessibility of an encapsulated compound is one of the best ways to assess if the encapsulation system will allow the bioactive compound available to be absorbed. The nanoparticle must be designed to reach the targeted tissues. Even though particles sized below

1000 nm are mentioned by several authors as nanoparticles, only the ones sized between 50 to 200 nm have shown results for effective delivery systems (Chow et al., 2015).

To quantify the amount of β-carotene that resists the gastrointestinal conditions, the INFOGEST *in vitro* simulation of gastrointestinal digestion protocol (Brodkorb et al., 2019a) was used and the bioaccessibility of BC loaded in two types of nanoparticles was determined.

The protocol evaluates the BC present in the micellar phase after digestion, representing the amount of bioactive compound accessible to be absorbed by the absorptive cells of the human intestine. BC is a hydrophobic lipophilic compound, thus, it needs to be incorporated into mixed micelles that pass through aqueous medium towards the target site. Efficient micellization of BC during digestion is crucial for BC bioaccessibility (WRIGHT et al., 2007).

The oral phase is meant to simulate the hydration and lubrication of food in the mouth in order to obtain a sufficient liquid input to facilitate mixing in the gastric phase. Therefore, this phase does not pose an influence on the digestion of the nanoparticles of both polymers. In the gastric phase, the bolus is diluted by simulated gastric fluids, pepsin is added, and the pH is adjusted to 3.0. In the intestinal phase, the chyme from the previous phase is mixed with bile and pancreatic juice. Bile is crucial to emulsify fat and form mixed micelles that transport BC through the intestinal epithelium (Brodkorb et al., 2019a).

In the present study, the concentration of BC initially used to digestion was 20 μg/mL. Considering that 5 mL of nanoparticles solution was used to perform the digestion procedure, 100 μg of BC was considered to be the initial mass of BC.

Table 3.4 shows the mass of BC determined in each phase considering a total volume of 20 mL or 40 mL for the gastric phase or intestinal phase, respectively.

For the determination of the bioaccessibility, two hypotheses are proposed: i) the extraction method allows recovering 100% meaning that the total amount of BC present in the sample is extracted, therefore the initial mass value for BC is 100 μg or ii) the extraction efficiency is lower than 100%, and the maximum amount of BC that is possible to extract from the initial (non-digested) samples is used. Therefore, the BC of non-digested samples of EC and zein was extracted to determine the extraction efficiencies.

Table 3.4. Mass of BC (μg) determined by HPLC after each digestion phase for EC or zein nanoparticles and a control sample of BC dissolved in sunflower oil

Samples	Mass of BC (μg)	
	Gastric	Intestinal
Free BC in oil	5.65 ± 2.06	10.33 ± 1.12
EC–BC	3.81 ± 0.08	11.78 ± 0.12
Zein–BC	4.07*	14.89 ± 0.45

*No standard deviation available, only one value was obtained because the other values were under the detection limit. The remaining results were performed in triplicate.

Extraction tests were performed on non-digested samples. The results are presented in Table E.1 (ANNEX E). Zein nanoparticles present a different behavior towards the extraction method when compared with the EC nanoparticles. The extraction efficiency obtained for zein nanoparticles was 25.87%, which is very low when compared to 100% obtained for EC nanoparticles. Different approaches followed to facilitate the BC release from the nanoparticles in order to increase the extraction efficiency (Table E.1 and Table E.2, ANNEX E). A protease (alcalase) or DMSO were used in an attempt to disintegrate protein nanoparticles. Different dilutions were also tested to evaluate whether the BC concentration was saturating the extraction solvent (hexane). However, none of the approaches resulted in higher extraction efficiency.

Table 3.5 presents the bioaccessibility considering that the extraction method can recover 100% of the BC.

Table 3.5. Bioaccessibility of BC, after each digestion phase, for EC or zein nanoparticles and a control sample of BC dissolved in sunflower oil, considering an extraction efficiency of 100%

Samples	Bioaccessibility (%)	
	Gastric	Intestinal
Free BC in oil	5.65 ± 2.06	10.33 ± 1.12
EC—BC	3.81 ± ± 0.08	11.78 ± 0.12
Zein—BC	4.07	14.89 ± 0.45

Nonetheless, the bioaccessibility was also calculated considering maximum amount of BC ($m_{initial}$), the one possible to extract from the initial (non-digested) samples. As expected, in this case superior values of bioaccessibility were obtained for zein nanoparticles, as shown in Table 3.6. EC nanoparticles only show a slight change due to the high extraction efficiency obtained for these particles.

Table 3.6. Bioaccessibility of BC, after each digestion phase, for EC or zein nanoparticles and a control sample of BC dissolved in sunflower oil, considering $m_{initial}$ the maximum amount of BC possible to extract from the initial (non-digested) samples.

Samples	Bioaccessibility (%)	
	Gastric	Intestinal
EC—BC	2.70 ± 0.06	8.33 ± 0.09
Zein—BC	10.11	37.00 ± 1.11

Moreover, the results obtained showed that the sample free BC in sunflower oil has an intestinal bioaccessibility of 10.33%. However, the sample evaluates the digestibility in oil and not water. Therefore, for the nanoparticles to be effective in the delivery of BC in the intestinal phase compared to BC in oil (highly soluble), higher bioaccessibility values would be desirable.

In general, EC nanoparticles revealed low bioaccessibility of BC. Indeed, EC is insoluble in water at any pH that occurs in the organisms, and during the digestion process there are no enzymes

able to digest EC. However it swells in the presence of gastric juice making it permeable for water and allowing BC to diffuse and be released (Wasilewska & Winnicka, 2019). For that reason, EC nanoparticles showed some BC release in the gastric phase (3.81 ± 0.08 μg, Table 3.4). However, this quantification in the gastric phase could also be due to the free non-encapsulated BC, since the encapsulation efficiency for EC-BC system is 66.56%, leaving 33.44% of BC in the free form, outside the particles, that could be detected after the gastric phase and so, it might not be as a result of the polymer digestion. However, chemical degradation of BC was also previously observed and associated to the enzyme activity (Patras et al., 2009). Thereby, BC degradation may also explain the low amount of BC detected.

Kim et al. (2017) reported that EC coatings are able to modify drug release by retarding it in the stomach and intestine, releasing the drug gradually in the colon. Drug release was impeded by the layer of EC, regardless of the acidity of the medium. In addition, Sadeghi et al. (2003) reported that EC drug release rate is greatly affected by the amount of polymer used in the matrices formed and decreased release rate was observed when polymer was increased.

In this work, ethylcellulose particles also have a higher ratio of polymer to BC compared to zein particles. A larger quantity of ethylcellulose was used to encapsulate the same amount of BC. Similar results were obtained by Sadeghi et al. (2003) when drug particles were incorporated in EC matrix which cause a great delay in drug diffusion through the polymer.

In zein nanoparticles, there is not a significant difference when compared to EC nanoparticles: in the gastric phase 4.07 μg of BC were detected for zein nanoparticles and 3.81 μg for the EC nanoparticles, and in the intestinal phase 11.78 μg of BC for EC nanoparticles and 14.89 μg detected for zein nanoparticles (Table 3.4). The results are not in accordance to previously reported studies where pepsin and pancreatin were able to digest protein (Chuacharoen & Sabliov, 2016). The low bioaccessibility obtained for the zein nanoparticles is probably related to the low zein solubility in aqueous medium, hampering the enzyme action. This phenomenon is supported by the ineffectiveness of the protease in the attempt to desintegrate the zein nanoparticles through enzymatic hydrolysis. Furthermore, some BC could still remain stuck to the zein nanoparticles due to hydrophobic interactions between BC and zein, since zein is an amphiphilic protein, which can cause higher resistance to the enzymatic hydrolysis (Chuacharoen & Sabliov, 2016).

Chuacharoen et al. (2016) demonstrated that BC nanoemulsions revealed improved bioacessibility compared with zein nanoparticles, since they are more susceptible to digestion. Thereby, zein

nanoparticles as a carrier system proved to protect BC for longer periods under the digestive conditions. In any case, BC loaded in zein nanoparticles could be improved by the presence of lipids in the food matrix, increasing BC solubility and bioaccessibility (Chuacharoen & Sabliov, 2016).

In general, even though the bioaccessibility of BC entrapped in both zein and EC was not much higher than the control sample in oil, both nanoparticles showed improved protection and less release in the gastric phase and higher release in the intestinal phase.

To sum up, the big difference in the analysis of zein nanoparticles is in the extraction efficiency to be considered. The bioaccessibility is higher (37%, Table 3.6.) if the maximum of BC that can be extracted is 25.89% versus the amount of BC obtained when considering 100% of extraction efficiency (14.89%, Table 3.5). Because there is a difficulty in extract all BC from zein, the recommended bioaccessibility approach would be to consider the extraction efficiency of 25.87%, because this value might also have been obtained in the extractions after digestion, even if the BC is in the mixed micelles. If, indeed, there is an interaction between zein and BC, this could also be present in the mixed micelles hindering the proper extraction of BC. Because zein is also insoluble in hexane and organic solvents, it can precipitate and hold the BC.

CHAPTER 4 CONCLUSIONS AND FUTURE WORK

The main aim of this study was the assessment of techniques for the scale-up production of polymeric nanoparticles, testing its feasibility at a lab-scale for the future application at an industrial scale. For the food industry, the scale-up factor is pertinent since an optimized large production is necessary considering the increasing demand for fortified food products.

This study highlights several methods for the productions of polymeric nanoparticles that are able to scale-up being the most promising method using the T-mixer device, following the solvent-displacement method. The device has been used previously to produce said polymeric nanoparticles and a pilot-scale can be optimized to produce up to 20-fold larger quantities compared to laboratory-scale.

The development and optimization of hydrophobic polymeric nanoparticles for the encapsulation of an insoluble lipophilic bioactive compound: β-carotene, using two different polymers: zein and ethylcellulose was executed at a laboratory-scale. β-carotene loaded zein or ethylcellulose nanoparticles were successfully produced using the solvent-displacement method. The nanoparticles presented spherical morphology and narrow size distributions with encapsulation efficiency of 92.59 and 66.56% for zein and ethylcellulose nanoparticles, respectively.

In vitro digestion study showed that both nanosystems are strongly insoluble in the digestion medium, hampering the action of the enzymes and salts to release the β-carotene from the nanoparticles. However, zein nanoparticles reveled higher β-carotene bioaccessibility. Both nanoparticles showed increased protection in the gastric phase and higher releases in the intestinal phase.

Opportunities can now arise in order to improve this work as follows:

- The simulation of a pilot-scale production using a T-mixer device, and optimization of the conditions of production;

- The operation of a dynamic gastro-intestinal simulation that would be able to simulate the stomach, duodenum, jejunum, ileum and colon to assess a more accurate bioaccessibility;

- To improve the bioaccessibility, the use of lecithin as a surfactant can help solubilize β-carotene and improve its incorporation in the mixed micelles;

- The investigation and optimization of new methods of extraction the allow the accurate way to quantify β-carotene;

- Increasing exposure of humans to nanosystems with its diverse properties demands to predict the toxicity and hazard capability of the produced nanoparticles as a method of characterization;

- The storage of the nanoparticles as a suspension can present several problems, among them is microbiological contaminations, polymer degradation, particle aggregation and sedimentation and the loss of the functionality of the bioactive compound. Therefore, the shift for another form is necessary. A form of powder by freeze-drying is a common technique and the insurance that the suspension is resuspendable without aggregation. Furthermore, freeze-drying compliments well this work because it can be used at an industrial scale.

REFERENCES

Agüeros Bazo, M., Esparza Catalán, I., González Ferrero, C., González Navarro, C. J., Irache Garreta, J. M., & Romo Hualde, A. (2016). *Patent No. US 9,381,252 B2*. Washington, DC.

Ahmed, B., Yusuf, M., Khan, M., & Khan, R. (2012). Plausible antioxidant biomechanics and anticonvulsant pharmacological activity of brain-targeted beta-carotene nanoparticles. *International Journal of Nanomedicine*, *7*, 4311. https://doi.org/10.2147/IJN.S34588

Albanes, D. (1999). β-Carotene and lung cancer: a case study. *The American Journal of Clinical Nutrition*, *69*(6), 1345S-1350S. https://doi.org/10.1093/ajcn/69.6.1345S

Alminger, M., Aura, A.-M., Bohn, T., Dufour, C., El, S. N., Gomes, A., … Santos, C. N. (2014). In Vitro Models for Studying Secondary Plant Metabolite Digestion and Bioaccessibility. *Comprehensive Reviews in Food Science and Food Safety*, *13*(4), 413–436.

Anderson, T. J., & Lamsal, B. P. (2011). REVIEW: Zein Extraction from Corn, Corn Products, and Coproducts and Modifications for Various Applications: A Review. *Cereal Chemistry Journal*, *88*(2), 159–173.

Avanço, G. B., & Braschi, M. L. (2008). Preparation and characterisation of ethylcellulose microparticles containing propolis. *Revista de Ciências Farmacêuticas Básica e Aplicada*, *29*(2), 129–135.

Barreras-Urbina, C. G., Ramírez-Wong, B., López-Ahumada, G. A., Burruel-Ibarra, S. E., Martínez-Cruz, O., Tapia-Hernández, J. A., & Félix, F. R. (2016). Nano- and Micro-Particles by Nanoprecipitation: Possible Application in the Food and Agricultural Industries. *International Journal of Food Properties*, *19*(9), 1912–1923.

Baudot, C., Tan, C. M., & Kong, J. C. (2010). FTIR spectroscopy as a tool for nano-material characterization. *Infrared Physics and Technology*, *53*(6), 434–438.

Boon, C. S., McClements, D. J., Weiss, J., & Decker, E. A. (2010). Factors Influencing the Chemical Stability of Carotenoids in Foods. *Critical Reviews in Food Science and Nutrition*, *50*(6), 515–532.

Briançon, S., Fessi, H., Lecomte, F., & Lieto, J. (1999). STUDY AND SCALE-UP OF A NANOPRECIPITATION PROCESS. In *14th International Symposium on Industrial Crystallization*. IChemE.

Brodkorb, A., Egger, L., Alminger, M., Alvito, P., Assunção, R., Ballance, S., … Recio, I. (2019a). INFOGEST static in vitro simulation of gastrointestinal food digestion. *Nature Protocols*, *14*(4), 991–1014. https://doi.org/10.1038/s41596-018-0119-1

Brodkorb, A., Egger, L., Alminger, M., Alvito, P., Assunção, R., Ballance, S., … Recio, I. (2019b). INFOGEST static in vitro simulation of gastrointestinal food digestion supplementary information. *Nature Protocols*, *14*(4), 991–1014.

Calderó, G., Leitner, S., García-Celma, M. J., & Solans, C. (2019). Modulating size and surface charge of ethylcellulose nanoparticles through the use of cationic nano-emulsion templates. *Carbohydrate Polymers*, *225*, 115201. https://doi.org/10.1016/j.carbpol.2019.115201

Charcosset, C., & Fessi, H. (2005). Preparation of nanoparticles with a membrane contactor.

Journal of Membrane Science, *266*(1–2), 115–120.

Chow, S. F., Wan, K. Y., Cheng, K. K., Wong, K. W., Sun, C. C., Baum, L., & Chow, A. H. L. (2015). Development of highly stabilized curcumin nanoparticles by flash nanoprecipitation and lyophilization. *European Journal of Pharmaceutics and Biopharmaceutics*, *94*, 436–449. https://doi.org/10.1016/j.ejpb.2015.06.022

Chuacharoen, T., & Sabliov, C. M. (2016). The potential of zein nanoparticles to protect entrapped β-carotene in the presence of milk under simulated gastrointestinal (GI) conditions. *LWT - Food Science and Technology*, *72*, 302–309.

Corradini, E., Curti, P., Meniqueti, A., Martins, A., Rubira, A., & Muniz, E. (2014). Recent Advances in Food-Packing, Pharmaceutical and Biomedical Applications of Zein and Zein-Based Materials. *International Journal of Molecular Sciences*, *15*(12), 22438–22470. https://doi.org/10.3390/ijms151222438

D'Addio, S. M., & Prud'homme, R. K. (2011). Controlling drug nanoparticle formation by rapid precipitation. *Advanced Drug Delivery Reviews*, *63*(6), 417–426.

Dasgupta, A., & Klein, K. (2014). *Antioxidants in foods, vitamins and suplements: Prevention and Treatment of Disease*. Academic Press.

de Freitas Zômpero, R. H., López-Rubio, A., de Pinho, S. C., Lagaron, J. M., & de la Torre, L. G. (2015). Hybrid encapsulation structures based on β-carotene-loaded nanoliposomes within electrospun fibers. *Colloids and Surfaces B: Biointerfaces*, *134*, 475–482. https://doi.org/10.1016/j.colsurfb.2015.03.015

Deng, X.-X., Chen, Z., Huang, Q., Fu, X., & Tang, C.-H. (2014). Spray-drying microencapsulation of β-carotene by soy protein isolate and/or OSA-modified starch. *Journal of Applied Polymer Science*, *131*(12).

European Comission. (2008). Regulation (EC) No 1333/2008 of the European Parliament and of the Council of 16 December 2008 on food additives. *Off J Eur Union*, (354), 16–33.

Fernandez, A., Torres-Giner, S., & Lagaron, J. M. (2009). Novel route to stabilization of bioactive antioxidants by encapsulation in electrospun fibers of zein prolamine. *Food Hydrocolloids*, *23*(5), 1427–1432.

Fessi, H., Puisieux, F., Devissaguet, J. P., Ammoury, N., & Benita, S. (1989). Nanocapsule formation by interfacial polymer deposition following solvent displacement. *International Journal of Pharmaceutics*, *55*(1), R1–R4. https://doi.org/10.1016/0378-5173(89)90281-0

Galindo-Rodríguez, S. A., Puel, F., Briançon, S., Allémann, E., Doelker, E., & Fessi, H. (2005). Comparative scale-up of three methods for producing ibuprofen-loaded nanoparticles. *European Journal of Pharmaceutical Sciences*, *25*(4–5), 357–367.

Gómez-Mascaraque, L. G., Perez-Masiá, R., González-Barrio, R., Periago, M. J., & López-Rubio, A. (2017). Potential of microencapsulation through emulsion-electrospraying to improve the bioaccesibility of β-carotene. *Food Hydrocolloids*, *73*, 1–12. https://doi.org/10.1016/j.foodhyd.2017.06.019

Gunstone, F. D. (2003). *Lipids for functional foods and nutraceuticals* (1st ed., Vol. 13). The Oily

Press.

Guo, J.-X., & Gray, D. G. (1994). Preparation, characterization, and mesophase formation of esters of ethylcellulose and methylcellulose. *Journal of Polymer Science Part A: Polymer Chemistry*, *32*(5), 889–896. https://doi.org/10.1002/pola.1994.080320510

Hayden, D. R., Kibbelaar, H. V. M., Imhof, A., & Velikov, K. P. (2018). Fully-biobased UV-absorbing nanoparticles from ethyl cellulose and zein for environmentally friendly photoprotection. *RSC Advances*, *8*(44), 25104–25111. https://doi.org/10.1039/C8RA02674B

Hedrén, E., Diaz, V., & Svanberg, U. (2002). Estimation of carotenoid accessibility from carrots determined by an in vitro digestion method. *European Journal of Clinical Nutrition*, *56*(5), 425–430.

Holding, D. R. (2014). Recent advances in the study of prolamin storage protein organization and function. *Frontiers in Plant Science*, *5*, 276. https://doi.org/10.3389/fpls.2014.00276

Horn, D., & Rieger, J. (2001). Organic Nanoparticles in the Aqueous Phase—Theory, Experiment, and Use. *Angewandte Chemie International Edition*, *40*(23), 4330–4361. https://doi.org/10.1002/1521-3773(20011203)40:23<4330::AID-ANIE4330>3.0.CO;2-W

Hurtado-López, P., & Murdan, S. (2005). Formulation and characterisation of zein microspheres as delivery vehicles. *Journal of Drug Delivery Science and Technology*, *15*(4), 267–272. https://doi.org/10.1016/S1773-2247(05)50048-0

Jain, A., Sharma, G., Kushwah, V., Ghoshal, G., Jain, A., Singh, B., … Katare, O. P. (2018). Beta carotene-loaded zein nanoparticles to improve the biopharmaceutical attributes and to abolish the toxicity of methotrexate: a preclinical study for breast cancer. *Artificial Cells, Nanomedicine, and Biotechnology*, *46*(sup1), 402–412. https://doi.org/10.1080/21691401.2018.1428811

Johnson, B. K., & Prud'homme, R. K. (2003). Chemical processing and micromixing in confined impinging jets. *AIChE Journal*, *49*(9), 2264–2282.

Kasaai, M. R. (2018). Zein and zein -based nano-materials for food and nutrition applications: A review. *Trends in Food Science and Technology*, *79*, 184–197.

Khan, S. A., Ahmad, M., Aamir, M. N., Murtaza, G., Rasool, F., & Akhtar, M. (2010). Study of Nimesulide Release From Ethylcellulose Microparticles and Drug- Study of Nimesulide Release From Ethylcellulose Microparticles and Drug-Polymer Compatibility Analysis. *Lat. Am. J. Pharm, 29*(4), 554–561.

Khayata, N., Abdelwahed, W., Chehna, M. F., Charcosset, C., & Fessi, H. (2012). Preparation of vitamin e loaded nanocapsules by the nanoprecipitation method: From laboratory scale to large scale using a membrane contactor. *International Journal of Pharmaceutics*, *423*(2), 419–427. https://doi.org/10.1016/j.ijpharm.2011.12.016

Kim, M. S., Yeom, D. W., Kim, S. R., Yoon, H. Y., Kim, C. H., Son, H. Y., … Choi, Y. W. (2016). Development of a chitosan based double layer-coated tablet as a platform for colon-specific drug delivery. *Drug Design, Development and Therapy*, *Volume11*, 45–57. https://doi.org/10.2147/DDDT.S123412

Lai, H. L., Pitt, K., & Craig, D. Q. M. (2010). Characterisation of the thermal properties of ethylcellulose using differential scanning and quasi-isothermal calorimetric approaches.

International Journal of Pharmaceutics, *386*(1–2), 178–184. https://doi.org/10.1016/j.ijpharm.2009.11.013

Leitner, S., Solans, C., García-Celma, M. J., & Calderó, G. (2019). Low-energy nano-emulsification approach as a simple strategy to prepare positively charged ethylcellulose nanoparticles. *Carbohydrate Polymers*, *205*, 117–124.

Lepeltier, E., Bourgaux, C., & Couvreur, P. (2014). Nanoprecipitation and the "Ouzo effect": Application to drug delivery devices. *Advanced Drug Delivery Reviews*, *71*, 86–97. https://doi.org/10.1016/j.addr.2013.12.009

Li, F., Chen, Y., Liu, S., Qi, J., Wang, W., Wang, C., … Zhang, Y. (2017). Size-controlled fabrication of zein nano/microparticles by modified anti-solvent precipitation with/without sodium caseinate. *International Journal of Nanomedicine*, *12*, 8197–8209. https://doi.org/10.2147/IJN.S143733

Lince, F., Marchisio, D. L., & Barresi, A. A. (2008). Strategies to control the particle size distribution of poly- ε -caprolactone nanoparticles for pharmaceutical applications. *Journal of Colloid and Interface Science*, *322*(2), 505–515.

Liu, Y., Cheng, C., Prud'homme, K. R., & Fox, R. O. (2008). Mixing in a multi-inlet vortex mixer (MIVM) for flash nano-precipitation. *Chemical Engineering Science*, *63*(11), 2829–2842.

Madni, A., Ekwal, M., Ahmad, S., Din, I., Hussain, Z., Ranjha, N., & Khan, M. I. (2014). FTIR Drug-Polymer Interactions Studies of Perindopril Erbumine FTIR Drug-Polymer Interactions Studies of Perindopril Erbumine. *Journal of the Chemical Society of Pakistan*, *36*(6).

Miladi, K., Sfar, S., Fessi, H., & Elaissari, A. (2016). Nanoprecipitation Process: From Particle Preparation to In Vivo Applications. In *Polymer Nanoparticles for Nanomedicines* (pp. 17–53). https://doi.org/10.1007/978-3-319-41421-8_2

Murtaza, G. (2012). Ethylcellulose microparticles: A review. *Acta Poloniae Pharmaceutica - Drug Research*, *69*(1), 11–22.

Neha, T., Shishir, T., & Ashutosh, D. (2017). Fourier transform infrared spectroscopy (FTIR) profiling of red pigment produced by Bacillus subtilis PD5. *African Journal of Biotechnology*, *16*(27), 1507–1512. https://doi.org/10.5897/AJB2017.15959

Packer, L., Kraemer, K., Obermüller-Jevic, U., & Sies, H. (2005). *Carotenoids and Retinoids: Molecular Aspects and Health Issues*. Champaing, Illinois: AOCS Publishing.

Paiva, S. A. R., & Russell, R. M. (1999). β-Carotene and Other Carotenoids as Antioxidants. *Journal of the American College of Nutrition*, *18*(5), 426–433.

Papalia, Í. da S., & Londero, P. M. G. (2015). Extração de zeína e sua aplicação na conservação dos alimentos. *Ciência Rural*, *45*(3), 552–559.

Penalva, R., Esparza, I., Agüeros, M., Gonzalez-Navarro, C. J., Gonzalez-Ferrero, C., & Irache, J. M. (2015). Casein nanoparticles as carriers for the oral delivery of folic acid. *Food Hydrocolloids*, *44*, 399–406.

Peñalva, R., Esparza, I., González-Navarro, C. J., Quincoces, G., Peñuelas, I., & Irache, J. M. (2015). Zein nanoparticles for oral folic acid delivery. *Journal of Drug Delivery Science and*

Technology, *30*, 450–457.

Penalva, R., González-Navarro, C. J., Gamazo, C., Esparza, I., & Irache, J. M. (2017). Zein nanoparticles for oral delivery of quercetin: Pharmacokinetic studies and preventive anti-inflammatory effects in a mouse model of endotoxemia. *Nanomedicine: Nanotechnology, Biology and Medicine*, *13*(1), 103–110. https://doi.org/10.1016/j.nano.2016.08.033

Pénicaud, C., Achir, N., Dhuique-Mayer, C., Dornier, M., & Bohuon, P. (2011). Degradation of β-carotene during fruit and vegetable processing or storage: reaction mechanisms and kinetic aspects: a review. *Fruits*, *66*(6), 417–440.

Pinto Reis, C., Neufeld, R. J., Ribeiro, A. J., & Veiga, F. (2006). Nanoencapsulation I. Methods for preparation of drug-loaded polymeric nanoparticles. *Nanomedicine: Nanotechnology, Biology and Medicine*, *2*(1), 8–21.

Porter, S. C. (1989). Controlled-Release Film Coatings Based on Ethylcellulose. *Drug Development and Industrial Pharmacy*, *15*(10), 1495–1521.

Qian, C., Decker, E. A., Xiao, H., & McClements, D. J. (2012). Nanoemulsion delivery systems: Influence of carrier oil on β-carotene bioaccessibility. *Food Chemistry*, *135*(3), 1440–1447.

Quintanar-Guerrero, D., Allémann, E., Fessi, H., & Doelker, E. (1998). Preparation Techniques and Mechanisms of Formation of Biodegradable Nanoparticles from Preformed Polymers. *Drug Development and Industrial Pharmacy*, *24*(12), 1113–1128.

Rama, K., Senapati, P., & Das, M. K. (2005). Formulation and in vitro evaluation of ethyl cellulose microspheres containing zidovudine. *Journal of Microencapsulation*, *22*(8), 863–876.

Rao, J. P., & Geckeler, K. E. (2011). Polymer nanoparticles: Preparation techniques and size-control parameters. *Progress in Polymer Science*, *36*(7), 887–913. https://doi.org/10.1016/j.progpolymsci.2011.01.001

Reimer, L. (2013). *Transmission electron microscopy: physics of image formation and microanalysis* (Vol. 36). Springer.

Rekhi, G. S., & Jambhekar, S. S. (1995). Ethylcellulose - A Polymer Review. *Drug Development and Industrial Pharmacy*, *21*(1), 61–77.

Ribeiro, H. S., Chu, B.-S., Ichikawa, S., & Nakajima, M. (2008). Preparation of nanodispersions containing β-carotene by solvent displacement method. *Food Hydrocolloids*, *22*(1), 12–17.

Rowe, R. C., Sheskey, P. J., & Quinn, M. E. (2009). *Handbook Pharmaceutical Excipients* (6th ed.). Pharmaceutical Press.

Sadeghi, F., Garekani, H. A., & Sadeghi, R. (2003). COMPARISON OF ETHYLCELLULOSE MATRIX CHARACTERISTICS PREPARED BY SOLID DISPERSION TECHNIQUE OR PHYSICAL MIXING. *DARU Journal of Pharmaceutical Sciences*, *11*(1), 7–3.

Sessa, D. J., Eller, F. J., Palmquist, D. E., & Lawton, J. W. (2003). Improved methods for decolorizing corn zein. *Industrial Crops and Products*, *18*(1), 55–65. https://doi.org/10.1016/S0926-6690(03)00033-5

Silva, H. D., Cerqueira, M. Â., & Vicente, A. A. (2012). Nanoemulsions for Food Applications:

Development and Characterization. *Food and Bioprocess Technology*, *5*(3), 854–867.

Swathi, P., & Krishna Sailaja, A. (2014). Formulation of ibuprofen loaded ethyl cellulose nanoparticles by nanoprecipitation technique. *Asian Journal of Pharmaceutical and Clinical Research*, *7*(3), 44–48.

Tao, J., Chow, S. F., & Zheng, Y. (2019). Application of flash nanoprecipitation to fabricate poorly water-soluble drug nanoparticles. *Acta Pharmaceutica Sinica B*, *9*(1), 4–18. https://doi.org/10.1016/j.apsb.2018.11.001

Tewa-Tagne, P., Briançon, S., & Fessi, H. (2007). Preparation of redispersible dry nanocapsules by means of spray-drying: Development and characterisation. *European Journal of Pharmaceutical Sciences*, *30*(2), 124–135.

U.S. Food & Drug Administration. (2019). CFR - Code of Federal Regulations Title 21: zein. Retrieved September 16, 2019, from https://www.accessdata.fda.gov/scripts/cdrh/cfdocs/cfcfr/CFRSearch.cfm?fr=184.1984

Urbán-Morlán, Z., Mendoza-Elvira, S. E., Hernández-Cerón, R. S., Alcalá-Alcalá, S., Ramírez-Mendoza, H., Ciprián-Carrasco, A., … Quintanar-Guerrero, D. (2015). Preparation of ethyl cellulose nanoparticles by Solvent-Displacement using the conventional method and a recirculation system. *Journal of the Mexican Chemical Society*, *59*(3), 173–180.

Valente, I., Celasco, E., Marchisio, D. L., & Barresi, A. A. (2012). Nanoprecipitation in confined impinging jets mixers: Production, characterization and scale-up of pegylated nanospheres and nanocapsules for pharmaceutical use. *Chemical Engineering Science*, *77*, 217–227.

Vauthier, C., & Bouchemal, K. (2009). Methods for the Preparation and Manufacture of Polymeric Nanoparticles. *Pharmaceutical Research*, *26*(5), 1025–1058.

Wan, Z.-L., Guo, J., & Yang, X.-Q. (2015). Plant protein-based delivery systems for bioactive ingredients in foods. *Food & Function*, *6*(9), 2876–2889.

Wang, M., Fu, Y., Chen, G., Shi, Y., Li, X., Zhang, H., & Shen, Y. (2018). Fabrication and characterization of carboxymethyl chitosan and tea polyphenols coating on zein nanoparticles to encapsulate β-carotene by anti-solvent precipitation method. *Food Hydrocolloids*, *77*, 577–587. https://doi.org/10.1016/j.foodhyd.2017.10.036

Wasilewska, K., & Winnicka, K. (2019). Ethylcellulose–A Pharmaceutical Excipient with Multidirectional Application in Drug Dosage Forms Development. *Materials*, *12*(20), 3386. https://doi.org/10.3390/ma12203386

WRIGHT, A., PIETRANGELO, C., & MACNAUGHTON, A. (2007). Influence of simulated upper intestinal parameters on the efficiency of beta carotene micellarisation using an in vitro model of digestion. *Food Chemistry*, *107*(3), 1253–1260. https://doi.org/10.1016/j.foodchem.2007.09.063

Xu, H., Jiang, Q., Reddy, N., & Yang, Y. (2011). Hollow nanoparticles from zein for potential medical applications. *Journal of Materials Chemistry*, *21*(45), 18227. https://doi.org/10.1039/c1jm11163a

Yi, J., Lam, T. I., Yokoyama, W., Cheng, L. W., & Zhong, F. (2015). Beta-carotene encapsulated in food protein nanoparticles reduces peroxyl radical oxidation in Caco-2 cells. *Food*

Hydrocolloids, *43*, 31–40. https://doi.org/10.1016/j.foodhyd.2014.04.028

Yin, L.-J., Chu, B.-S., Kobayashi, I., & Nakajima, M. (2009). Performance of selected emulsifiers and their combinations in the preparation of β-carotene nanodispersions. *Food Hydrocolloids*, *23*(6), 1617–1622.

Zhang, Y., Cui, L., Che, X., Zhang, H., Shi, N., Li, C., … Kong, W. (2015). Zein-based films and their usage for controlled delivery: Origin, classes and current landscape. *Journal of Controlled Release*, *206*, 206–219. https://doi.org/10.1016/j.jconrel.2015.03.030

Zhang, Y., Cui, L., Chen, Y., Zhang, H., Zhong, J., Sun, Y., … Kong, W. (2015). Zein-Based Nanofibres for Drug Delivery: Classes and Current Applications. *Current Pharmaceutical Design*, *21*(22), 3199–3207.

Zhang, Y., Cui, L., Li, F., Shi, N., Li, C., Yu, X., … Kong, W. (2016). Design, fabrication and biomedical applications of zein-based nano/micro-carrier systems. *International Journal of Pharmaceutics*, *513*(1–2), 191–210. https://doi.org/10.1016/j.ijpharm.2016.09.023

ANNEXES

Annex A Optimization of nanoparticle's parameters

I. Ethylcellulose nanoparticles experimental design

Table A.1. Tested formulations assayed for the production of blank ethylcellulose nanoparticles

EC concentration (organic phase) (%)	Antisolvent concentration (%)	Size by intensity (nm)	Size by number (nm)	PDI
0.1	60	163.57	109.81	0.201
0.1	80	103.18	68.47	0.287
0.2	70	182.75	126.98	0.153
0.4	60	258.29	176.31	0.242
0.4	80	187.47	127.58	0.253

Table A.2. Concentrations tested for BC loaded nanoparticles of 0.1% ethylcellulose and 80% of antisolvent concentration

BC concentration (%)	Size by intensity (nm)	Size by number (nm)	PDI
0.04	ND*	ND	> 0.5
0.02	ND	ND	> 0.5
0.01	ND	ND	> 0.5
0.005	ND	ND	> 0.5
0.001	ND	ND	> 0.5
0.0004	109.06	75.62	0.369
0.0001	112.23	69.86	0.213
0.00004	105.82	73.56	0.259
0.00005	101.80	63.12	0.315
0.00008	111.85	76.82	0.244

* ND – non detectable

II. Zein nanoparticles experimental design

Table A.3. Tested formulations assayed for the production of blank zein nanoparticles

Zein concentration (%)	Antisolvent concentration (%)	Flow rate (ml/min)	Size by intensity (nm)	Size by number (nm)	PDI
0.4	80	0.3	131.04	88.90	0.214
0.4	80	0.7	136.74	133.42	0.195
0.4	90	0.3	90.98	63.90	0.226
0.4	90	0.7	95.47	66.84	0.285
0.6	85	0.5	128.37	82.87	0.222
0.8	80	0.3	156.06	104.44	0.181
0.8	80	0.7	162.28	112.0	0.213
0.8	90	0.3	104.5	74.42	0.243
0.8	90	0.7	104.1	70.14	0.290

Table A.4. Different concentrations tested for BC loaded nanoparticles of 0.4% zein, 90% of antisolvent concentration and 0.7 ml/min flow rate

BC concentration (%)	Size by intensity (nm)	Size by number (nm)	PDI
0.04	81.72	62.75	> 0.5
0.02	114.29	85.82	> 0.5
0.005	72.17	58.10	> 0.5
0.001	94.38	66.43	0.233
0.0005	83.91	61.26	0.211

Annex B Calibration Curve of BC

Table B.1. Dilutions and respective absorbances measured at λ=453 nm for the calibration curve

BC concentration (%)	0.000008	0.00002	0.00006	0.0001	0.0005	0.001
Dilution	1/125	1/50	1/16.67	1/10	1/2	1
Absorbance	0.010	0.009	0.026	0.044	0.173	0.323

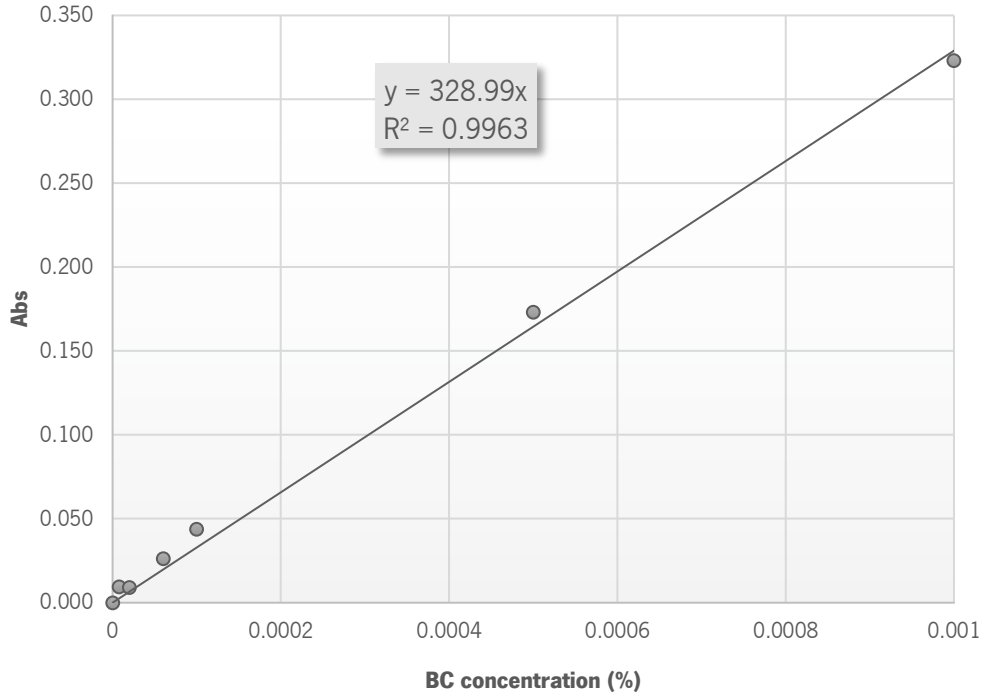

Figure B.1. Calibration curve for β-carotene diluted in ethanol.

Annex C Enzyme activities and bile concentration assays

I. Pepsin activity assay

Table C.1. Results from the pepsin activity assay

Sample (μg/ml)	Abs (Blank-Sample)	Activity (Units/mg)
5	0.136	2720
10	0.269	2690
15	0.434	2893.3
20	0.542	2710
25	0.782	3128
30	0.960	3200
	Average	**2890.2**

II. Trypsin from pancreatin activity assay

Table C.2. Results from the trypsin from pancreatin activity assay

Concentration	Linear regression equation	Quantity of pancreatin (mg)	Activity (Units/mg)
Blank	y = 0.0003x + 1.6401	-	-
0.1 mg/ml	y = 0.0114x + 1.6413	0.01	6.17
0.5 mg/ml	y = 0.0501x + 1.6984	0.05	5.53
1 mg/ml	y = 0.0819x + 1.7411	0.1	4.53
		Average	**5.41**

III. Bile concentration assay

Table C.3. Results from bile concentration assay

Concentration (mg/ml)	Dilution factor	Fluorescence intensity			Bile (mM)
		Sample	Internal Standard	Sample blank	
0.06	1000	39725	43308	6412	87.86
0.03	2000	29055.5	38451.5	6321.5	96.78
0.01	6000	12638.5	22212	5747	86.38
				Average	**90.34**

Annex D HPLC calibration curve

Table D.1. Dilutions and area under the curve measured at λ=450 nm for the HPLC calibration curve of BC

BC concentration (μg/mL)	Dilution	Area under curve
25	0	4635.50
12.5	1/2	2313.70
6.25	1/4	1107.50
3.13	1/8	527.40
2.5	1/10	406.10
1.56	1/16	262.30
1.25	1/20	190.90
0.63	1/40	96.30
0.31	1/80	49.50
0.16	1/160	26.90

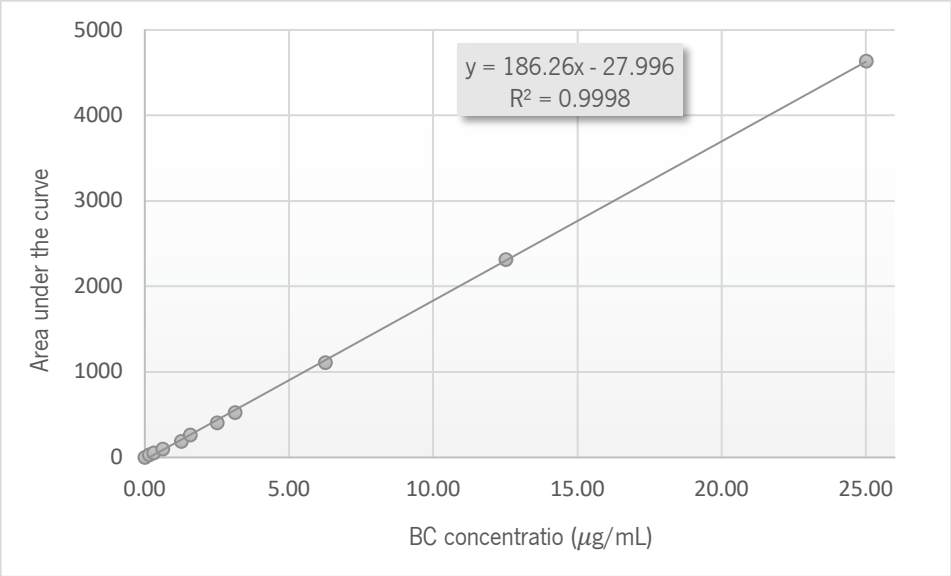

Figure D.1. Calibration curve for β-carotene analyzed by HPLC.

Annex E Extraction efficiency assays

Table E.1. Concentrations and extraction efficiencies obtained for BC loaded zein and EC nanoparticles and with protein degradation methods on the zein particles; considering BC initial concentration of 20 µg/mL

Sample	Concentration after extraction (µg/mL)	Extraction efficiency (%)
EC-BC	28.29 ± 0.93	>100
Zein-BC	5.17 ± 0.21	25.87
Protease	5.04 ± 0.94	25.22
DMSO	4.96 ± 0.39	24.81

Table E.2. Extraction efficiencies obtained for non-digested BC loaded zein nanoparticles for different dilutions

BC initial concentration (µg/mL)	Dilution	Concentration after extraction (µg/mL)	Extraction efficiency (%)
20	-	5.17 ± 0.21	25.87
10	1/2	5.74 ± 0.26	28.70
5	1/4	6.47 ± 0.42	32.35
2.5	1/8	6.90 ± 0.15	34.50